ingegneria sismica
International Journal of Earthquake Engineering
Anno XXXVI – Num.1

# SEISMIC RETROFITTING OF CONFINED MASONRY-RC BUILDINGS: THE CASE STUDY OF THE UNIVERSITY HALL OF RESIDENCE IN MESSINA, ITALY

*Dario De Domenico[1], Nicola Impollonia[2], Giuseppe Ricciardi[1]*

[1] Department of Engineering, University of Messina, Italy

[2]Department of Civil Engineering and Architecture, University of Catania, Italy

SUMMARY: *Several buildings located in earthquake-prone areas were conceived according to past design guidelines and do not comply with current seismic regulations. This requires effective seismic retrofitting interventions. After the collapse of the university hall of residence of L'Aquila, Italy, in 2009, several regional authorities in other Italian cities planned surveys for seismic assessments of similar student accommodation buildings, disclosing dramatic structural deficiencies in many cases. One of these buildings concerns the student hall of residence of Messina, Italy, a confined masonry-RC building analysed in this paper. This work summarizes the theoretical conception and underlying design philosophy of the seismic retrofitting of this building (through buckling restrained braces and pre-tensioned steel ribbons), describes the pushover analysis on the original and retrofitted structure, illustrates the acceptance tests on the hysteretic dampers performed at laboratory CERISI of Messina and discusses some construction issues that have arisen up to date during the installation phases.*

KEYWORDS: *seismic retrofit, hysteretic dampers, buckling restrained braces, pre-tensioned stainless steel ribbons, confined masonry building*

## 1 Introduction

Seismic retrofitting of existing buildings is a challenging task that requires effective, economical and feasible strategies depending on the different structural typologies. The need of seismic retrofitting of existing buildings located in high-hazard earthquake areas may arise for different circumstances. For example, the map of seismic hazard is continuously evolving and it is very likely that the current peak ground acceleration (PGA) of a particular installation site, as prescribed by seismic regulations in force today, is higher than in the past. Additionally, many concepts of modern seismic design like ultimate limit states and capacity design principles have been implemented in seismic standards only in quite recent times, and were entirely unknown when these buildings were originally constructed. Another possible motivation for seismic retrofitting is related to the increase of an importance class of a given building, which automatically implies higher seismic demand.

In line with these motivations and of particular relevance to the present contribution, the 2008 Italian seismic code [D.M. 2008, NTC 08] dramatically increased the seismic hazard level in most Italian regions, which implies that the safety of a large number of existing buildings is to be re-checked in view of these updated regulations. Consequently, it emerges that a large number of buildings do not meet the current seismic regulations and requires seismic retrofitting interventions because they are not able to resist the design earthquake-induced forces any longer. Priority should be given to those buildings having high importance factor,

Corresponding author: Dario De Domenico, Department of Engineering, University of Messina, Italy.
Email: dario.dedomenico@unime.it

meaning that their function is of key importance for social and economic reasons (hospitals, schools, fire stations, university buildings, etc.). There are two main strategies of seismic retrofitting: 1) strengthening the existing structure by increasing the load-bearing capacity of each structural member and/or 2) modifying the seismic performance of the building by introducing seismic protection devices like base isolators and/or supplemental energy dissipation devices. The literature regarding structural control strategies is quite vast, ranging from review papers on the subject [Zhou et al., 2002; Spencer Jr. and Nagarajaiah 2003; Symans et al., 2008] to discussion of analysis methods and case studies [Oliveto and Marletta, 2005] involving traditional and innovative seismic retrofitting techniques of existing reinforced concrete (RC) buildings, including base isolation [Ferraioli and Mandara, 2016; Ferraioli and Mandara, 2017; De Domenico and Ricciardi, 2018a,b; De Domenico et al., 2018a,b; Castaldo et al., 2015], energy dissipation devices e.g. fluid viscous dampers [De Domenico and Ricciardi, 2019], dissipation braces [Bruno and Valente, 2002; Longo et al. 2015] and buckling restrained braces [Di Sarno and Manfredi, 2010], with specific reference not only to structural elements but also to non-structural components [Gandelli et al., 2018]. The above list of papers is far from being exhaustive. Strengthening option alone may be expensive and sometimes unfeasible for very large buildings, since this type of intervention would involve a large number of structural elements (beams, columns). Some interferences with non-structural components may additionally discourage such a strengthening intervention when applied throughout the structure. This is why in several practical situations dampers or seismic base isolators are resorted to for a more effective retrofitting intervention, in conjunction with local repairing and/or strengthening operations limited to critical zones of the structure that are particularly weak and vulnerable to the earthquake-induced lateral forces. Thus, local strengthening techniques can be combined with seismic protection devices for a more effective retrofitting intervention. The case study building described in this paper represents an emblematic example of such a combined retrofitting intervention, as clarified below.

After the tragic collapse of the university hall of residence of L'Aquila, Italy, due to the 2009 earthquake, several local or regional authorities in other Italian cities were strongly motivated to perform seismic assessment of similar student accommodation buildings, disclosing dramatic structural deficiencies in many cases. One of these buildings, the student hall of residence of the University of Messina, Italy, represents the case study discussed in the present paper. Built in 1930, the so-called "Casa dello Studente" has been used until nowadays as the main university hall of residence of Messina. It is worth reminding that the city of Messina experienced one of the most catastrophic earthquake events of modern history: the 7.1 Mw 1908 Messina earthquake and the concurrent tsunami caused more than 100000 deaths and destroyed at least 91% of structures in Messina. The first four stories of the case study building were made of confined brick masonry, with confining RC beams and columns that were casted in a later stage than the masonry walls. This structural configuration was developed and extensively adopted as construction scheme of several buildings that were erected in Messina after the above-mentioned 1908 earthquake. Instead, the last two elevations (fifth floor and an overlying light appendage) were built almost 40 years later (in the early 70s) in typical RC frame. Besides this structural heterogeneity in elevation, the building is also non-symmetric in plan, with a typical C shape characterized by a long front side and two shorter wings. Therefore, the building is non-regular in elevation and non-symmetric in plan, proving to be rather vulnerable to horizontal ground motion accelerations. The above-mentioned updated (increased) seismic demands for the installation site prescribed by the new Italian seismic

standards [D.M. 2008, NTC 08] have required urgent seismic retrofitting interventions in order to keep the building operational.
The adopted retrofitting solution consists of buckling restrained braces that replace the masonry walls of the original building at all the five stories but only in some specific frames of the overall 3D structure, which were selected to minimize the torsional effects while increasing the overall dissipation capacity. These hysteretic dampers, representing supplemental energy dissipation devices, are combined with local strengthening interventions performed in the RC beam-to-column joints of the last floor through pre-tensioned stainless steel ribbons, which were designed to increase the ductility of the reinforced concrete frame by offering a beneficial triaxial compression stress state. The authors believe that, considering the historical value and the peculiar structural configuration of this building, the seismic retrofitting interventions could represent an interesting case study. Aim of this paper is to describe the main phases of this seismic retrofitting, including its theoretical conception and underlying design philosophy, the pushover analysis on the original and retrofitted structure, the acceptance tests carried out on the hysteretic dampers at the laboratory CERISI [Failla et al., 2015] of the University of Messina, and some construction issues that have arisen up to date during the installation stages.

## 2 Description of the case study building

The case study building "Casa dello Studente" represents the main student hall of residence of the University of Messina, Italy. From the aerial and plan views shown in Figure 1 (A, B) we note that the building has a C shape. In the internal courtyard another building ("Mensa" building) was realized quite recently but it is structurally independent and separated by a seismic joint. Located in the city center, this building has five stories, each one with an average area of around 1300m$^2$, and a light appendage at the fifth elevation (i.e., a floor built only in a restricted zone of the plan area). The original structure of only four stories (basement, ground floor, first and second floors) was built in 1932 in brick masonry confined by collaborating RC beams and columns. The fifth story (third floor) and the light appendage of the building, highlighted in red in the front views of Figure 1 (C, D), were erected around 40 years later than the original masonry building (approximately in the early 70s) through a typical RC frame scheme. The reinforcement bars of the added story in the RC frame were welded to the bars of the column of the underlying story in the masonry building. The internal partitions of the last two stories were realized through hollow brick masonry walls as in typical RC framed structures.

### 2.1 Historical background

After the 28 December 1908 earthquake in the city of Messina, new seismic regulations were issued. Among these, the regulations R.D. n. 2089 (23/10/1924) [Regio Decreto, 1924] prescribed limitations on the height of the buildings, and introduced guidelines for the construction of earthquake resistant structures, including the confined masonry system adopted in the case study building under study. Some additional details on this system are worth being reported here, since this represented one of the most widespread construction schemes in the re-construction of the city of Messina after the 1908 earthquake and extensively adopted until the Second World War. Considering the typical collapse of masonry buildings after the Messina earthquake, as shown in the photographs reported in Figure 2 (A, B), a hybrid collaborating masonry-RC system was developed to prevent the overturning of the masonry walls by increasing their out-of-plane resistance. Some peculiar aspects of this hybrid system

are sketched in Figure 2 (C, D). As a first step, the masonry walls were built with brick courses left staggered along the wall height. Reinforcing bars were concurrently prepared for the columns, which were casted in a later stage than the masonry walls.

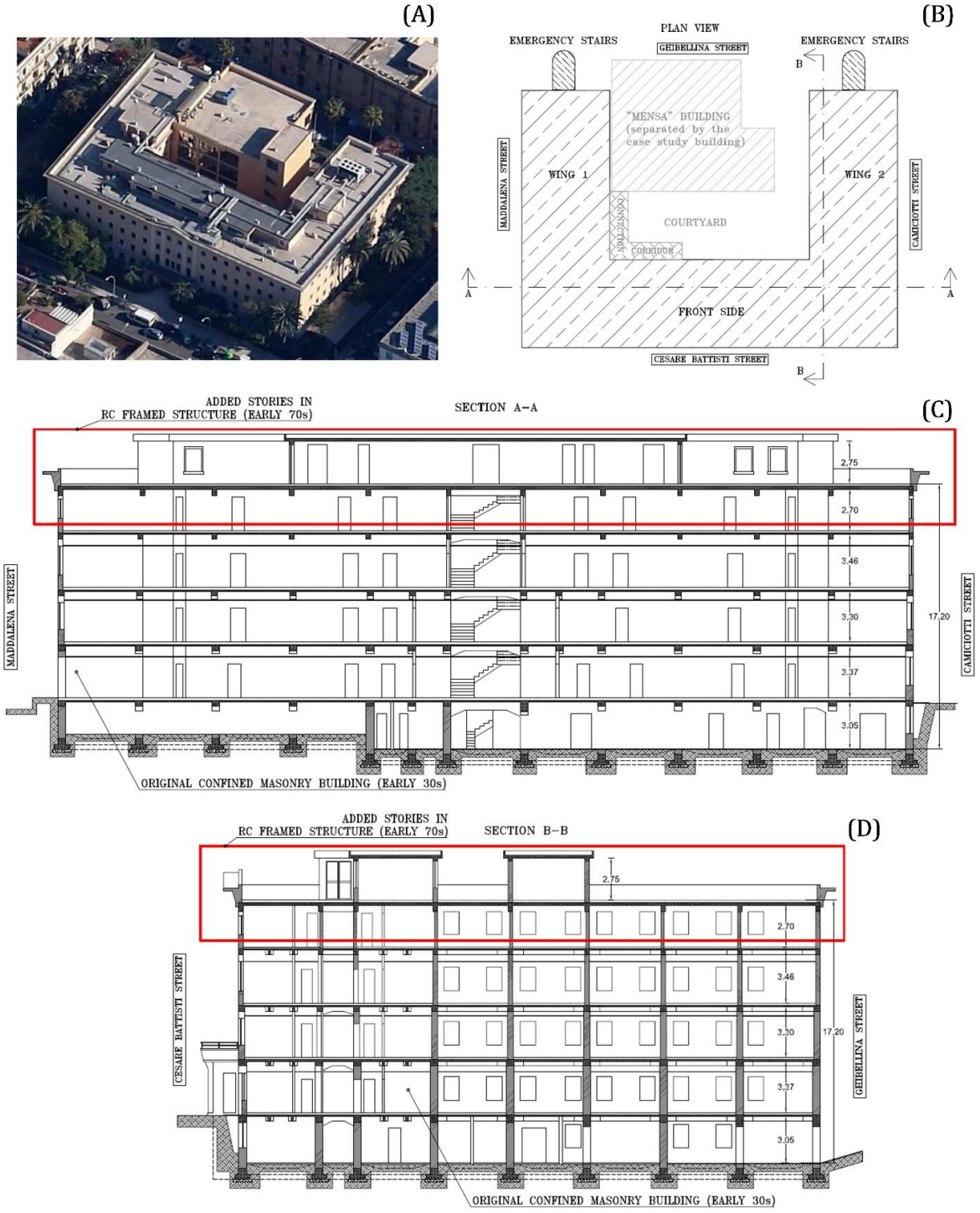


Figure 1 - *Case study building "Casa dello Studente": (A) aereal view; (B) plan view; (C) and (D) front views (section A-A and B-B, respectively) with added reinforced concrete stories highlighted in red*

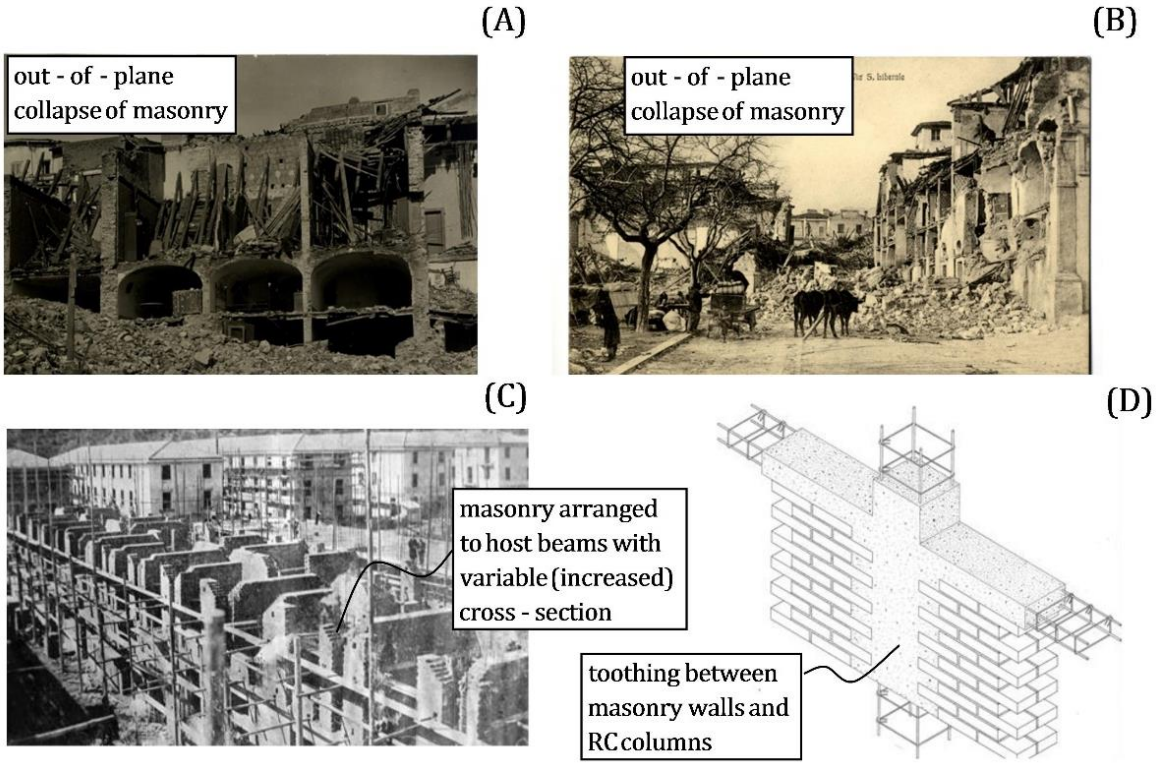


Figure 2 - *Out-of-plane collapse of masonry buildings in the Messina 1908 earthquake (A), (B), and typical structural scheme adopted in the re-construction of the city with masonry walls and confining (collaborating) RC beams and columns casted in a later stage than the masonry walls (C), (D)*

The staggered bricks of the walls allowed an effective toothing (structural collaboration) between masonry walls and RC columns. The masonry walls were subsequently exploited as formwork of the overlying RC beams. Moreover, in Figure 2 (C) it can be seen that the walls near the beam-column joints were sometimes arranged to host beams with variable (increased) section, which were quite popular in the past (and also pertinent to the case study building discussed in this paper). The resulting scheme turns out to be a hybrid masonry-RC structure, with mutual collaboration of two systems even for very small displacements, featuring a box-shaped configuration, desirable for an effective seismic behavior of the building. It is worth pointing out that, as better specified in the sequel of the paper, the compressive strength of concrete and the reinforcement amount of both RC columns and beams in the first four stories (relevant to the confined masonry scheme) were far lower than in a typical RC frame of modern constructions. Indeed, their presence was primarily for confining purposes of the masonry walls rather than to form the main structural system, and this is the key difference in comparison with a conventional (modern) RC frame with hollow brick masonry walls as perimeter infills and internal partitions (Asteris et al., 2011).

As to the identification of the geotechnical characteristics of the installation site, two continuous surveys (up to 30m depth), twenty-four standard penetration tests (with intervals of 2.50m depth) and one MASW (Multichannel Analysis of Surface Waves) data acquisition were performed. The results indicate that the installation site can be classified as a soil type B in accordance with the NTC08 seismic regulations ($360m/s < V_{s30} < 800m/s$), namely “deposits of very dense sand, gravel, or very stiff clay, at least several tens of meters in thickness, showing a gradual increase of mechanical properties with depth”.

## 2.2 Identification of structural details and reinforcement arrangement

A series of surveys *in situ* were carried out in order to determine the dimensions of the structural elements. The following tests were performed to identify the structural details and reinforcement arrangements:

- 48 extractions of concrete core cylinder samples, 24 on columns and 24 on beams, which were subject to laboratory compression tests up to failure;
- 20 extractions of steel bars, 10 on columns and 10 on beams, which were subject to laboratory tensile tests up to failure;
- 46 pull-out tests, 23 on columns and 23 on beams, which were used to identify the compressive strength of concrete through correlation empirical expressions.

The results of these tests were processed statistically in order to determine the mean values of compressive strength for concrete $R_{ck}$ and the mean tensile strength of steel (yield and rupture stress $f_y$ and $f_u$), which are reported in Table 1.

Table 1 - *Compressive strength $R_{ck}$ of concrete cores and tensile stress of steel bars (yield $f_y$ and rupture $f_u$ stress) extracted in situ and tested in laboratory*

| Elevation | $R_{ck}$ [MPa] columns | | | $R_{ck}$ [MPa] beams | | | $f_y$ [MPa] | $f_u$ [MPa] |
|---|---|---|---|---|---|---|---|---|
| | min | average | max | min | average | max | average | average |
| 1-4 (confined masonry) | 13.2 | 13.9 | 16.1 | 12.8 | 14.2 | 17.3 | 222.8 | 332.3 |
| 5,6 (added RC stories) | 16.3 | 18.9 | 23.1 | 17.2 | 20.7 | 28.3 | 301.9 | 482.0 |

The cross-section of the RC columns elements reduces from 50x50 cm (basement floor) to 30x30 cm for the top floor, as reported in Table 2. The beam cross-sections vary along the building height, from 50x70 cm down to 30x40 cm. The thicknesses of the masonry walls reduce from 50 cm (basement and ground floor) to 30 cm (second floor). As to the foundation system, the building was based on a typical RC strip foundation with inverted T-beams connected to each other along two main directions. The first four floor slabs were made of reinforced concrete plate 8cm thick stiffened by RC beams at a spacing of 1.50m, while the last two floors were made in typical one-way slab in reinforced concrete with hollow bricks as internal lightening elements. The original documentations of the building, in terms of reinforcement arrangement in the RC members, were found only for the last two elevations (added RC framed structure). Therefore, a set of simulated calculations (according to the regulations in force at that time [Regio Decreto, 1924]) were performed to identify the most reasonable reinforcement amount of beams and columns in the first four floors.

Table 2 - *Dimensions of RC columns and beams and masonry wall thicknesses*

| Level | RC columns $b \times h$ [cm] | RC beams $b \times h$ [cm] | Masonry wall $t$ [cm] |
|---|---|---|---|
| Foundation | - | 50 x 70 | - |
| Basement | 50 x 50 | 50 x 50 | 50 |
| Ground floor | 50 x 50 | 50 x 40 | 50 |
| First floor | 45 x 45 | 40 x 45 | 40 |
| Second floor | 35 x 40 | 30 x 45 | 30 |
| Third floor (added in a later stage) | 35 x 40; 35 x 30 | 30 x 60; 50 x 19 | - |
| Fourth floor (light appendage) | 30 x 30 | 30 x 40 | |

For these simulations, Aq42 steel (with admissible tensile stress equal to 1600kg/cm$^2$) and concrete Rck150 (with admissible compressive stress of 50kg/cm$^2$) were adopted.
According the mentioned seismic regulations R.D. n. 2089 [Regio Decreto, 1924], the following guidelines have been adopted in the simulated calculations:

- The vertical actions, permanent and variable, are increased up to 50% to account for the dynamic effects induced by the vertical component of the earthquake excitation;
- The design earthquake-induced lateral loads are assumed as 1/6 of the floor masses;
- The beams are designed under pure bending induced by the vertical loads (amplified by 50% as safety factor, in accordance with [Regio Decreto, 1924]);
- The columns are designed under the above-mentioned horizontal loads, considering a planar frame for each main direction of the building.

Two RC frames have been considered in the simulated calculations, one on the main front side (RC frame 2-105 composed of 13 spans), and one on the wing side of the building (RC frame 6-31 composed of 3 spans). The considered frames are highlighted in red in Figure 3. The considered vertical loads consist of a permanent load due to the self-weight equal to 450 kg/m$^2$ for every floor and a variable load of 300 kg/m$^2$ for first three floors and equal of 150 kg/m$^2$ for the last floor. The floor masses used for the assessment of the earthquake-induced lateral loads on the frames are listed in Table 3. The evaluation of the design bending moment was performed considering a fixed-fixed scheme to maximize the value at the two beam-ends, and a partially restrained scheme to maximize the value at the beam mid-span – cf. Table 4.

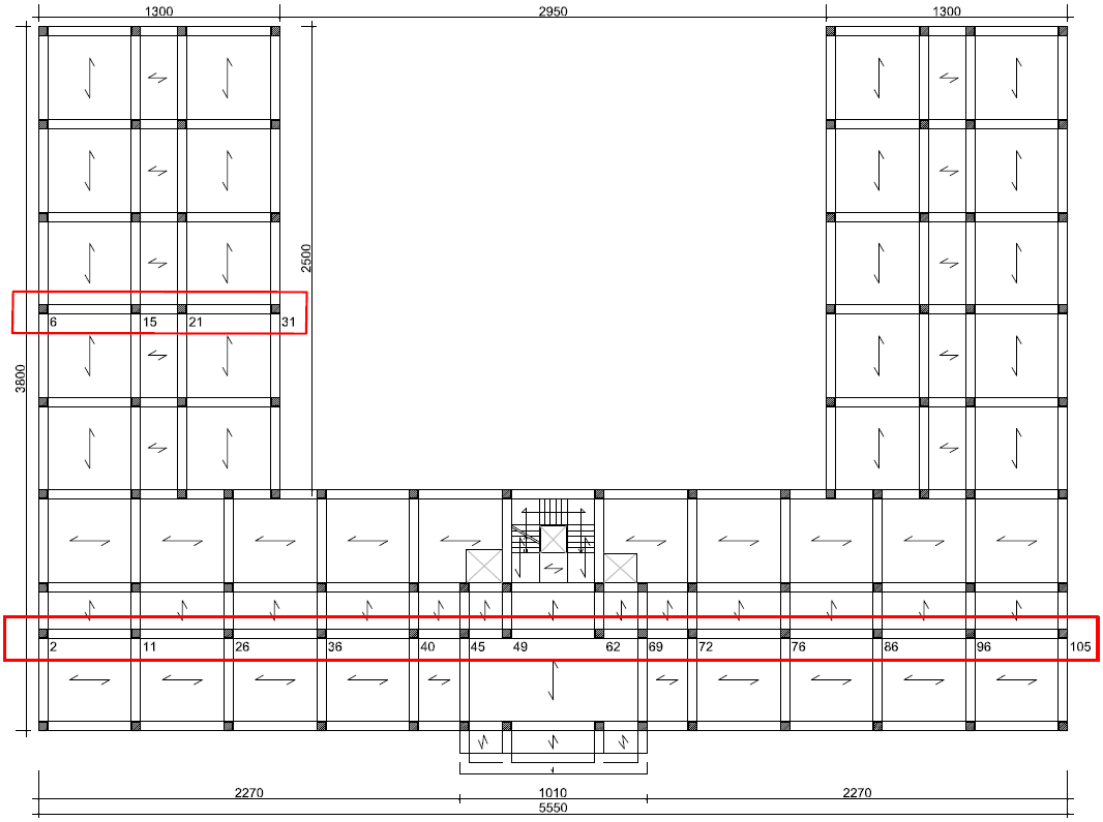


Figure 3 - *Plan view of the first floor of the building, the frames highlighted in red are those analyzed in the simulated calculations for the assessment of the reinforcement arrangement*

Reinforcement bars computed for the RC columns are listed in Table 5. For the reinforcement arrangement of the beams, we considered the presence of both straight bars and inclined (shaped) bars of common use at the time of the building construction, and stirrups made of 6mm diameter bars placed at 25cm spacing. For the reinforcement arrangement of the columns, we considered at least four bars at the corners of the section (with minimum diameter 20 mm for the top floor – cf. Table 5) and stirrups ϕ6@25 cm spacing like for the beams. These estimates of reinforcing bars were subsequently validated through pachometer (rebar locator) experimental measurements, as well as visual inspection of the bars after removal of the concrete cover in a few selected RC members – cf. Figure 4. These comparisons demonstrated a consistency of the actual re-bars in situ and the reinforcement bars obtained through the simulated calculations, as well as a perfect correspondence with the seismic prescriptions of the regulations of that time in terms of structural details and geometrical requirements.
Overall, according to the paragraph 8.5.4 of the Italian seismic code [D.M. 2008, NTC 08], based on the surveys and structural details acquired during the inspections, a knowledge level LC2 was achieved. This level corresponds to a confidence factor (FC) equal to 1.20, which has to be used for reducing the design strength parameters of the materials (reported above) to perform the structural verification of the existing building.

Table 3 - *Floor masses used for the earthquake-induced lateral loads in the simulated calculations*

| RC frame | Level | Floor slab mass [kg] | RC columns mass [kg] | RC beams mass [kg] | Masonry walls mass [kg] | Total floor mass [kg] |
|---|---|---|---|---|---|---|
| 2-105 | Basement | 6445 | 3965 | 4297 | 17438 | 32145 |
| | Ground floor | 6445 | 3541 | 3438 | 13950 | 27374 |
| | First floor | 6445 | 2706 | 3094 | 10463 | 22708 |
| | Second floor | 5156 | 1133 | 2320 | - | 8609 |
| 6-31 | Basement | 5859 | 1133 | 977 | 3488 | 11457 |
| | Ground floor | 5859 | 1012 | 781 | 2790 | 10442 |
| | First floor | 5859 | 773 | 703 | 2700 | 10035 |
| | Second floor | 4688 | 324 | 527 | - | 5539 |

Table 4 - *Simulated calculations of the reinforcement bars for the beams in the 2-105 frame, first floor*

| RC beam | section at the two beam-ends | | | | section at the beam mid-span | | | |
|---|---|---|---|---|---|---|---|---|
| | bending moment† | reinforcement area required | re-bars required | | bending moment† | reinforcement area required | re-bars required | |
| | $1.5\times\frac{ql^2}{12}$ [kg m] | $A_{s,req}$ [mm$^2$] | ϕ [mm] | n. bar | $1.5\times\frac{ql^2}{10}$ [kg m] | $A_{s,req}$ [mm$^2$] | ϕ [mm] | n. bar |
| 2-40 | 13602 | 2010 | 26 | 4 | 16322 | 2412 | 26 | 5 |
| 40-45 | 3966 | 586 | 26 | 2 | 4759 | 703 | 26 | 2 |
| 45-49 | 1033 | 153 | 26 | 1 | 1240 | 183 | 26 | 1 |
| 49-62 | 4883 | 721 | 26 | 2 | 5859 | 866 | 26 | 2 |
| 62-69 | 1033 | 153 | 26 | 1 | 1240 | 183 | 26 | 1 |
| 69-72 | 3966 | 586 | 26 | 2 | 4759 | 703 | 26 | 2 |
| 72-105 | 13602 | 2010 | 26 | 4 | 16322 | 2412 | 26 | 5 |

†A fixed-fixed scheme and a partially restrained scheme have been adopted to maximize the value of the bending moment at the beam ends and at the beam mid-span, respectively

Table 5 - *Simulated calculations of the reinforcement bars for the columns in the 6-31 frame*

| RC column | elevation | axial force | bending moment | column height | reinforcement area required | re-bars required | |
|---|---|---|---|---|---|---|---|
| | | $N$ [kg] | $M$ [kg m] | $H$ [cm] | $A_{s,req}$ [mm$^2$] | ϕ [mm] | n. bar |
| 6 | 1 | 14226.21 | 19289.64 | 50 | 2850 | 26 | 6 |
| 6 | 2 | 7743.03 | 7746.33 | 50 | 1145 | 26 | 3 |
| 6 | 3 | 3751.61 | 5846.84 | 45 | 967 | 24 | 3 |
| 6 | 4 | 972.78 | 4536.00 | 40 | 851 | 20 | 3 |
| 15 | 1 | 19879.61 | 22790.74 | 50 | 3367 | 26 | 7 |
| 15 | 2 | 10569.97 | 17446.23 | 50 | 2578 | 26 | 5 |
| 15 | 3 | 3277.42 | 10628.20 | 45 | 1757 | 24 | 4 |
| 15 | 4 | 204.7 | 3726.80 | 40 | 699 | 20 | 3 |
| 21 | 1 | 19914.01 | 22790.72 | 50 | 3367 | 26 | 6 |
| 21 | 2 | 10604.16 | 17446.46 | 50 | 2578 | 26 | 5 |
| 21 | 3 | 3313.85 | 10634.06 | 45 | 1758 | 24 | 4 |
| 21 | 4 | 228.23 | 3692.69 | 40 | 693 | 20 | 3 |
| 31 | 1 | 14191.8 | 19291.20 | 50 | 2850 | 26 | 6 |
| 31 | 2 | 7708.84 | 7741.95 | 50 | 1144 | 26 | 3 |
| 31 | 3 | 3715.19 | 5908.30 | 45 | 977 | 24 | 3 |
| 31 | 4 | 949.25 | 3260.96 | 40 | 612 | 20 | 2 |

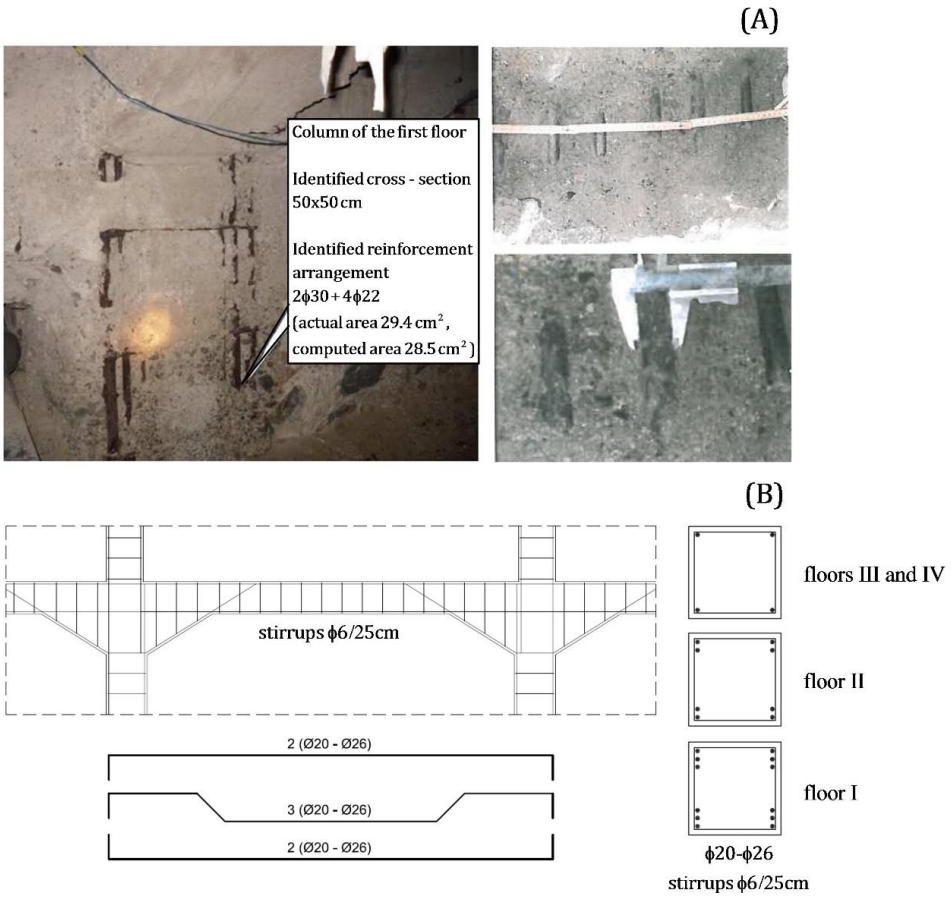


Figure 4 - *Identification of reinforcement bars in RC beams and columns through visual inspections (A) and simulated calculations (B)*

## 3 Seismic performance of existing building

The seismic performance of the case study building prior to retrofitting interventions has been assessed through static nonlinear analysis (pushover analysis – N2 method) [Fajfar, 2000]. The prescriptions of the NTC08 [D.M. 2008, NTC 08] have been followed. The structure is modeled with the design loads reported in the Italian seismic code, based on the functions and intended use of the building. As to the earthquake-induced design loads, the case study building is located in the high-hazard earthquake area of Messina, Italy. Therefore, the seismic action is evaluated based on the local hazard, and considering an importance factor relevant to class III ($C_u$=1.5), which is relevant to significant crowding [D.M. 2008, NTC 08]. The corresponding reference life of the building is calculated as $V_R = V_N \times C_U = 50 \times 1.5 = 75\text{years}$ according to [D.M. 2008, NTC 08]. Two elastic pseudo-acceleration response spectra for the installation site are shown in Figure 5. These two response spectra, whose acronyms are SLD and SLV in [D.M. 2008, NTC 08], correspond to two different limit states that are associated with reference probability of exceedance equal to 63% and 10% in the reference life of the building, respectively. The two corresponding PGA values are 0.102g and 0.296g. The SLD and SLV limit states are approximately equivalent to the damage limitation requirement and no-collapse requirement of the Eurocode 8 [Eurocode 8, 2004].

The structure has been modeled through a three-dimensional finite element model (FEM), as shown in Figure 6. A diaphragm constraint has been applied at each floor to simulate the behavior of a rigid floor. Despite the peculiar C shape of the building exhibiting a long front side and two shorter wings, it was preliminarily verified that the in-plane stiffness of the existing floors (8cm thick plates stiffened by RC beams at a spacing of 1.50m for the first three elevations and conventional RC one-way slab for the last two elevations) was large enough to guarantee compliance with the prescriptions of the NTC08 [D.M. 2008, NTC 08] and Eurocode 8 § 4.3.1 [Eurocode 8, 2004] about the rigidity of the diaphragm. For the application of the N2 method, the nonlinear force-deformation relationships for structural elements under monotonic loading are necessary [Fajfar, 2000]. The brick masonry walls are modeled through equivalent pin-jointed struts (resisting compression only) according to a simplified macro-modeling approach. There are many empirical expressions characterizing the structural behavior of such equivalent strut depending on the actual masonry geometrical and mechanical properties (see e.g. [Asteris, 2011; Tarque et al., 2015; De Domenico et al., 2018c]).

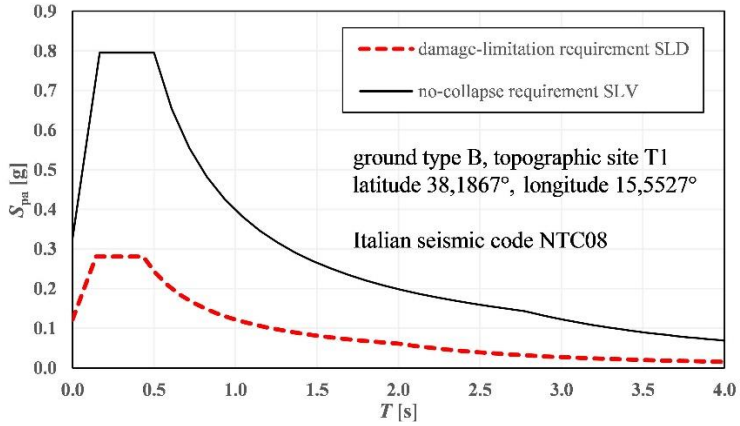


Figure 5 - *Pseudo-acceleration response spectrum for the installation site at different limit states (SLD: comparable to "damage limitation requirement"; SLV: comparable to "no-collapse requirement")*

In this paper the simplified approach suggested by the Italian guidelines [Circ. Min. 1997] has been adopted. According to this simplified approach, the nonlinear behavior of the masonry wall is approximated as an idealized elastoplastic curve with elastic stiffness $k_w$, ultimate strength $F_{u,w}$, yield displacement $\delta_{y,w}$ and ultimate displacement $\delta_{u,w}$, according to the following expressions [Circ. Min. 1997]:

$$
\begin{aligned}
&k_{\text{strut}} = 0.1 E_w t_w \ \text{(lateral stiffness of the equivalent strut)} \\
&k_w = k_{\text{strut}} \cos^2 \alpha \ \text{(lateral stiffness of the masonry wall)} \\
&F_{u,w} = \frac{f_{vk0} \, \text{l} \, t_w}{0.6} \ \text{(ultimate strength of the masonry wall)} \\
&\delta_{y,w} = \frac{F_{u,w}}{k_w} \ \text{(yield displacement of the masonry wall)} \\
&\delta_{u,w} = 0.004 h \ \text{(assumed ultimate displacement of the masonry wall)}
\end{aligned}
\tag{1}
$$

where $E_w$ denotes the Young's modulus of the masonry, $f_{vk0}$ is the shear strength of the masonry in the absence of vertical loads, $t_w$ represents the wall thickness and the other geometrical parameters $\text{l}, h, \alpha$ are indicated in the sketch of Figure 6.

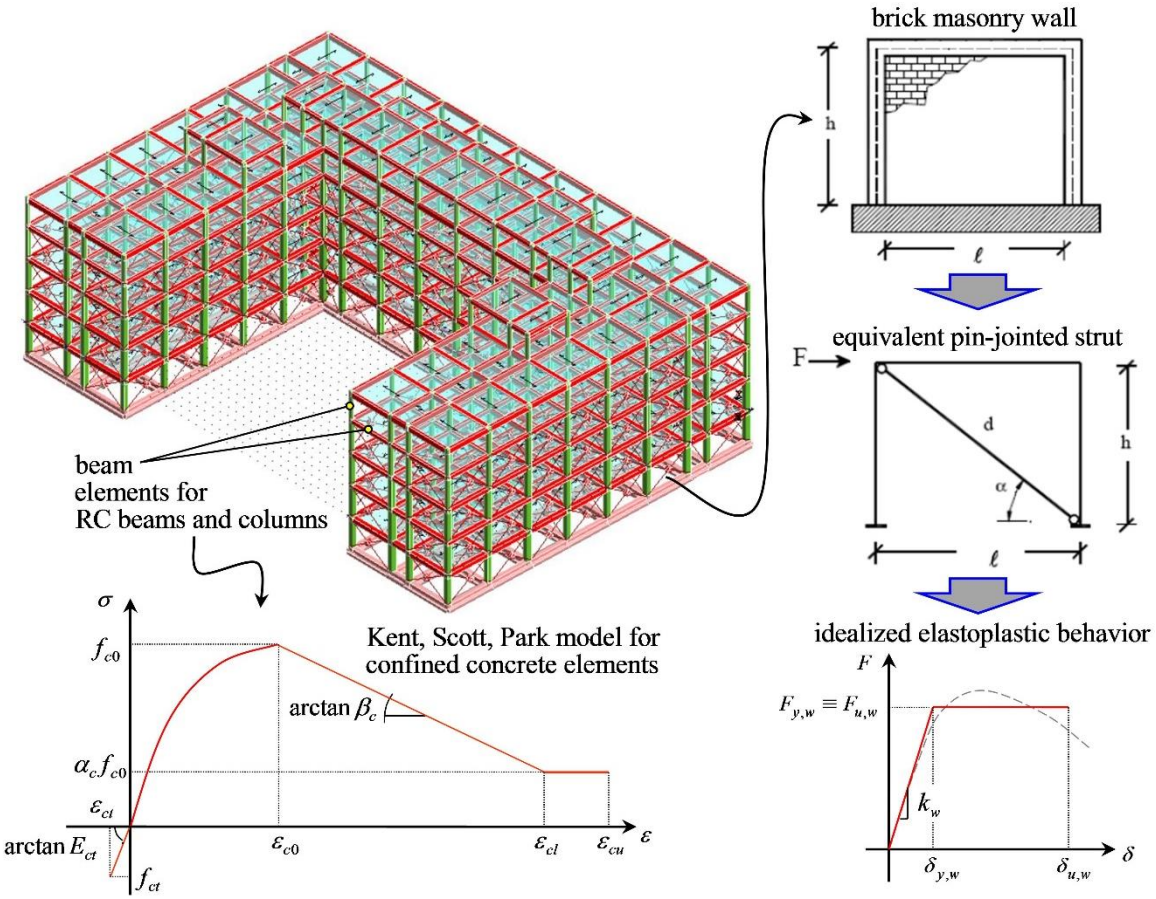


Figure 6 - *Finite element model of the case study building and simplified modeling assumptions for the brick masonry walls through an equivalent pin-jointed strut (macro-modeling approach)*

The resulting parameters of the elastoplastic model for the masonry walls are listed in Table 6. It is worth recognizing the limitations of the proposed model in comparison with more sophisticated models for brick masonry walls that are available in the literature and that were developed as improvements of the original model proposed in the 1960s [Polyakov, 1960]. As an example, models with more than just a single strut (multiple strut models) are better able to capture the interaction between the infill wall and the shear response of the column [Crisafulli et al., 2000]. Additionally, it was demonstrated that the vertical loads may have a certain influence on the evaluation of the strut width [Cavaleri et al., 2005; Amato et al., 2008]. Models involving concentric and eccentric struts have also been developed to describe the local effects induced by the interaction between masonry infill and surrounding frame [Al-Chaar, 2002]. Moreover, the strut width could also incorporate different constitutive behaviours depending on the load level, for instance depending on whether the panel is cracked or uncracked [Decanini and Fantin, 1987], or adopting a nonlinear response in compression, tension and shear [Crisafulli and Carr, 2007]. This is just a short list of papers regarding the several variants and improvements of the strut model, which outlines the complexity of the problem. Nevertheless, these more sophisticated analytical formulations may require additional variables and parameters that might not be reliably known in a seismic retrofitting process.

Table 6 - *Parameters of the masonry idealized elastoplastic behavior according to the macro-modeling approach (with* $l = 500$ cm*)*

| Level | masonry type | $f_{vk0}$ $\left[\frac{\text{kg}}{\text{cm}^2}\right]$ | $E_w$ $\left[\frac{\text{kg}}{\text{cm}^2}\right]$ | $h$ [cm] | $t_w$ [cm] | $k_w$ $\left[\frac{\text{kg}}{\text{cm}}\right]$ | $F_{u,w}$ [kg] | $\delta_{y,w}$ [cm] | $\delta_{u,w}$ [cm] |
|---|---|---|---|---|---|---|---|---|---|
| Basement | stone masonry | 0.6 | 10000 | 290 | 50 | 37414 | 25000 | 0.67 | 1.16 |
| Ground floor | brick masonry | 1.2 | 18000 | 300 | 50 | 66176 | 50000 | 0.76 | 1.20 |
| First floor | brick masonry | 1.2 | 18000 | 310 | 40 | 52008 | 40000 | 0.77 | 1.24 |
| Second floor | brick masonry | 1.2 | 18000 | 325 | 30 | 37961 | 30000 | 0.79 | 1.30 |

Beam elements with 6 DOFs are adopted for RC beams and columns. Beam elements with concentrated plasticity at both ends have been considered (plastic hinge approach). The Kent & Park model [Kent and Park, 1971] modified by Scott et al. [Scott et al., 1982] has been adopted to incorporate the confinement effect induced by the steel stirrups on the stress-strain confined concrete curve. The stress-strain relationship is described by

$$f_c = \begin{cases} [2(\varepsilon / \varepsilon_{c0}) - (\varepsilon / \varepsilon_{c0})^2] f_{c0} & 0 \le \varepsilon \le \varepsilon_{c0} \\ [1 - \beta_c (\varepsilon - \varepsilon_{c0})] f_{c0} & \varepsilon_{c0} \le \varepsilon \le \varepsilon_{cl} \\ \alpha_c f_{c0} & \varepsilon_{cl} \le \varepsilon \le \varepsilon_{cu} \end{cases} \quad (2)$$

where $f_{c0} = k\, f_c^{'}$ is the maximum stress of confined concrete ( $f_c^{'}$ being the maximum cylindrical stress of unconfined concrete) corresponding to a strain equal to $\varepsilon_{c0} = 0.002\,k$ , and $k$ represents a factor accounting for the confinement effect due to the transverse reinforcement expressed as

$$k = 1 + \frac{\rho_{sh} f_{yh}}{f_c^{'}} \geq 1 \tag{3}$$

with $\rho_{sh}$ being the ratio of the transverse reinforcement ratio (ratio of the confinement reinforcing bars and the confined concrete core) and $f_{yh}$ denoting the yield stress of the stirrups. The descending branch of the stress-strain curve is governed by the parameter

$$\beta_c = 0.5\left( \frac{3 + 0.29\, f_c^{'}}{145\, f_c^{'} - 1000} + 0.75\rho_{sh}\sqrt{\frac{p}{\Delta_{sh}}} - 0.002k \right)^{-1} \tag{4}$$

where $p$ denotes the width of the confined concrete core, and $\Delta_{sh}$ represents the stirrups spacing. The strain $\varepsilon_{cl}$ and the ultimate strain $\varepsilon_{cu}$ are expressed by, respectively

$$\varepsilon_{cl} = \varepsilon_{c0} + \frac{1-\alpha_c}{\beta_c}; \qquad \varepsilon_{cu} = 0.004 + 0.9\rho_{sh}\frac{f_{yh}}{300}. \tag{5}$$

The nonlinear behavior of the steel re-bars is finally described through a conventional bilinear elastoplastic model with strain hardening, as prescribed by the Italian seismic code [D.M. 2008, NTC 08].

The structure is subject to the above-mentioned vertical loads and a monotonically increasing pattern of lateral loads representing the earthquake-induced inertial forces. In line with the prescriptions of the Italian seismic code [D.M. 2008, NTC 08] two load distributions along the building height are considered: the first is proportional to the first modal shape ("mode-distribution") and the second is proportional to the mass distribution ("mass-proportional distribution"). A series of 16 combinations of pushover analysis have been performed, including four directions of the ground motion (±*x* and ±*y*), two lateral load distributions (mode- and mass-proportional distribution) and two additional eccentricities (±5% to the main plan dimension of the building). According to the N2 method, from the base-shear versus roof (top) displacement curve, an equivalent single-degree-of-freedom (SDOF) model is identified through a bilinear idealization of the pushover curve along with energy equivalence [Fajfar, 2000]. Then, the seismic demand (from the response spectrum of the installation site) is compared with the seismic capacity (from the resulting SDOF pushover curve). The results in terms of $\mathrm{PGA}_{\mathrm{capacity}} / \mathrm{PGA}_{\mathrm{demand}}$ for the most unfavourable combinations, among the 16 design scenarios, are as follows: for SLD ("damage limitation requirement" with return period 75 years) the lowest ratio $\mathrm{PGA}_{\mathrm{capacity}} / \mathrm{PGA}_{\mathrm{demand}} = 0.536$ ; for SLV ("no-collapse requirement" with return period 712 years) the lowest ratio $\mathrm{PGA}_{\mathrm{capacity}} / \mathrm{PGA}_{\mathrm{demand}} = 0.200$ . Therefore, in both cases the structure is not safe since its displacement capacity is lower than the displacement demand. Considering the very low $\mathrm{PGA}_{\mathrm{capacity}} / \mathrm{PGA}_{\mathrm{demand}}$ ratios obtained in the

two design scenarios (especially in the "no-collapse requirement" scenario), and the importance of the building related to its intended use as main student hall of residence, an effective seismic retrofitting intervention turns out to be necessary.

## 4 Seismic retrofitting operations

The most critical aspects identified by the analysis of the existing building are summarized below:

- the foundation structures fail due to shear failure, thus the cross-section of the inverted T-beams is inadequate to resist the design loads;
- the building exhibits a moderate torsional behavior due to the asymmetry in one direction (along the *x* axis), which gives rise to higher stresses in the structural elements along the perimeter of the building;
- the dissipation capacity of the building is unsatisfactory due to the very weak RC sections in beams and columns, which present very low reinforcement amounts and, thus, very low ductility, and the absence of the capacity design principles at the time of construction.

In order to retrofit the foundation, a set of RC plates have been designed to be added and connected to the existing inverted T-beams. This intervention, whose details are sketched in Figure 7, increases the stiffness and strength of the foundation so as to resist the seismic design loads. This intervention also leads to a reduction of the differential settlements and spreads the loads over a wider distribution area in a uniform manner. Design drawings and photographs taken in situ of the foundation retrofitting are reported in Figure 7. The intervention implies the elimination of the floors, followed by the removal of concrete cover, the placement of new reinforcement bars of the RC plate and connection to the existing T-beams through rheoplastic resin, and final casting of concrete. As said above, the existing RC beams and columns are structurally deficient because of the low mechanical strength of the employed materials and the low amount of transverse reinforcement. In particular, they are adequate to resist the vertical loads, but are unsatisfactory against the earthquake-induced lateral forces. Moreover, the asymmetry in plan leads to torsional effects under horizontal loads.
Motivated by these circumstances, buckling restrained braces (BRBs) have been designed for the retrofitting operations of the case study building. BRBs provide both stiffness and strength and have been designed to align the centre of mass (CM) with the centre of stiffness (CS), thus minimizing the torsional effects of the C-shaped building. The dissipation capacity of the hysteretic dampers related to the BRBs provide supplemental energy dissipation capability, thus reducing the stresses in the structural elements of the building. BRBs have been inserted in some specified locations (frames) from the foundation level up to the top floor. A series of steel frames are designed and developed to host the BRBs and to connect them with the existing structure, as shown below. These BRBs totally replace the confined masonry walls of the original building in the selected frames where they are installed. Finally, the beam-column joints of the fifth elevation (third floor) have been reinforced through pre-tensioned stainless steel ribbons, by offering a beneficial triaxial compression stress state. Indeed, these zones are particularly critical due to the different nature of the fifth story RC frame (added in a later stage than the original structure) in comparison with the underlying masonry building.

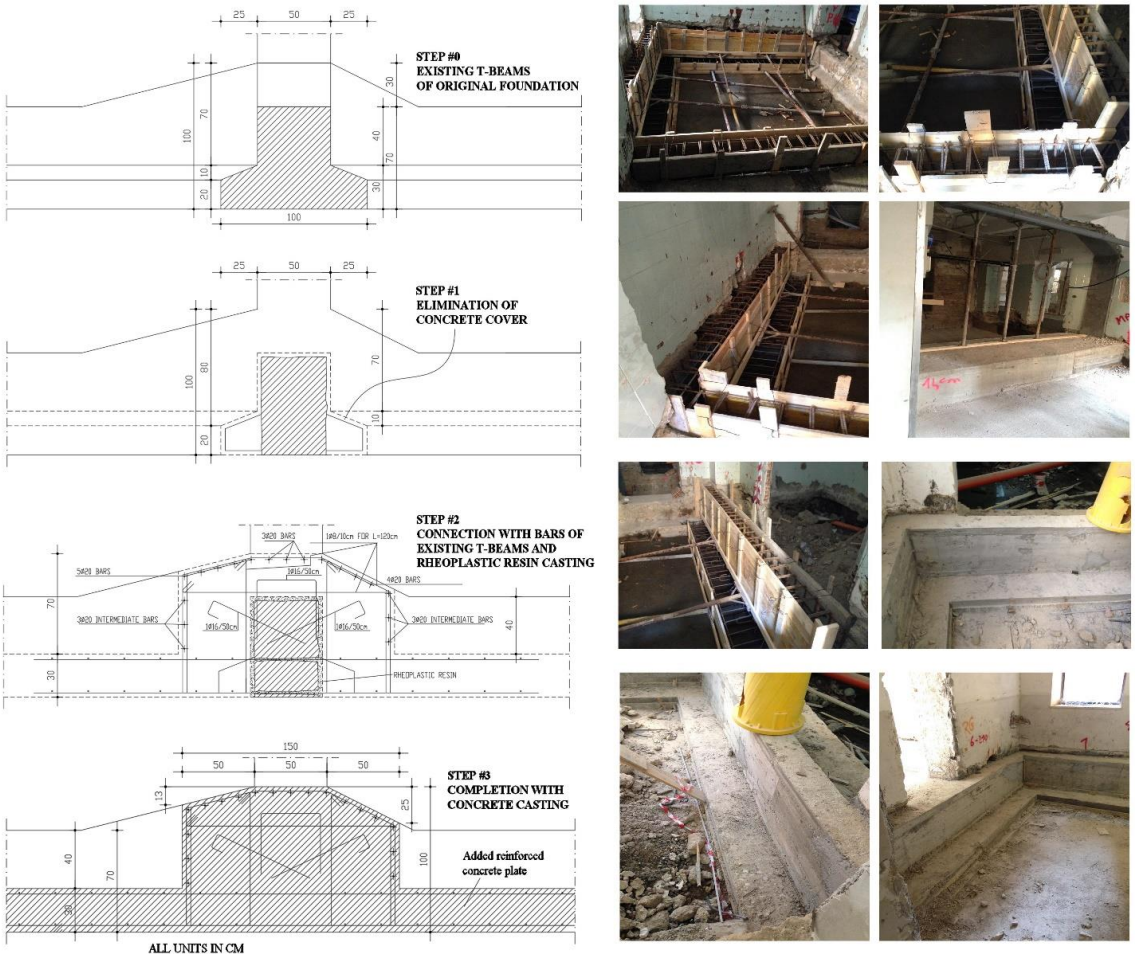


Figure 7 - *Retrofitting of foundation: design drawings (left) and photographs taken in situ (right)*

## 4.1 Design of hysteretic dampers and placement of BRBs

The choice of adopting BRBs is motivated by the stiff structure of the confined masonry-RC building. Indeed, the original structure, whose fundamental period is in the range of 0.4 s, undergoes very small displacements and, thus, the use of alternative supplemental energy dissipation devices like fluid viscous dampers [Soong and Dargush, 1997; Sorace and Terenzi, 2001; Tubaldi et al., 2014; De Domenico and Ricciardi, 2019] may be not very effective, as they would not be fully engaged due to the small interstory drifts experienced during the seismic event. On the contrary, the plastic deformation and dissipation capacity of BRBs can be activated even for small displacements, as the yield displacement of the internal element (an appropriately shaped steel plate) can be designed to be of few millimeters, which make them particularly suitable for stiff structures like the case study building.

Nowadays, the technology of BRBs [Kersting et al., 2015] is quite mature due to the several applications worldwide, especially for steel structures in Japan [Xie, 2005] and, subsequently, in the United States [Sabelli et al., 2003; Black et al., 2004; Tremblay et al., 2006]. The early principles date back to the early 70s, but devices with a stable force-deformation curve (i.e., with compressive yield strength equal to tensile yield strength) were developed and tested in the 80s and followings years [Watanabe et al., 1988; Wada and Nakashima, 2004] when first

experiments demonstrated the excellent dissipation capacity and ductility of concrete-filled steel tubes. BRBs consists of a steel core element, which is designed to carry the axial force. Thus, the dissipation features of these BRBs are of hysteretic nature, being based on the plastic deformation and yielding of the internal steel core in both tension and compression. Unlike other hysteretic devices that are subject to bending deformation, in BRBs there is no need of changing the cross-section (to promote yielding) as the plastic axial deformation is uniform in the entire section. However, the main problem to face is the risk of buckling for high compressive loads and in the presence of slender steel elements. Therefore, the steel plate is jacketed by a steel tube filled with concrete or grout in order to prevent buckling and to guarantee a stable (symmetric) cyclic force-displacement behavior in both tension and compressive regime. The steel core is axially disconnected from the filling material through specific (low-friction) coating materials that prevent the transmission of axial forces. After yielding of the steel core has occurred, the brace undergoes large deformation without decreasing its strength.

The design of BRBs in the confined masonry-RC structure under study has required a careful selection of the frames where the devices are to be installed. The selected frames are illustrated in Figure 8.


Figure 8 - *Selected frames for placement of BRBs (to minimize the distance between centre of mass and centre of stiffness, thus reducing the torsional effects under earthquake-induced lateral loads)*

These frames have been chosen with the aim to reduce eccentricities between the CM and the CS, thus minimizing the torsional effects of the building under earthquake-induced lateral loads. Indeed, while the building is symmetric with respect to the *y*-axis, it exhibits a torsional coupled behavior when subject to lateral components along the *x*-axis due its U-shape in plan. As can be seen from Figure 8, the BRBs are mostly concentrated near the two wings of the building to compensate for the different stiffness distribution on that side. The resulting mode shapes (first three modes) of the retrofitted building are depicted in Figure 9 and compared with those of the original building, wherein the translation of the CS towards the CM operated by the BRBs is clearly highlighted.

It can be noted that the first modal shape in the retrofitted building is almost purely translational, in contrast to the coupled torsional-translational nature of the same mode in the original building. Values of the modal participating mass ratios for the first three modes of vibration are also shown in Figure 9, while the first 12 periods, modal masses and participating mass ratios are listed in Table 7 and Table 8 for the existing building and retrofitted building, respectively. It is worth noting that for the existing building the first mode of vibration contributes to more than 75% of the modal mass for the *y* direction (due to the almost symmetrical configuration in that direction) but not for the *x* direction (wherein torsional coupled behavior occurs due to its U-shape in plan).

This requires careful selection of the load distribution in the pushover analysis, as the first mode distribution is not applicable in such cases [D.M. 2008, NTC08]. A procedure that accounts for the higher mode effects in both plan and elevation was proposed by Kreslin and Fajfar [Kreslin and Fajfar, 2012] and is adopted in the analysis of the existing building by considering correction factors arising from the elastic modal analysis. Nonlinear torsional effects and multimodal and adaptive pushover procedures were discussed, among others, in [De Stefano and Pintucchi, 2008; Ferraioli et al., 2016; Colajanni et al., 2017; Ferraioli et al., 2018]. On the other hand, the participating mass ratio for the first mode in the retrofitted building is slightly higher than 75% in both directions, thus the first mode distribution is applicable. The later force at each floor is roughly estimated through the well-known formula of the equivalent static linear analysis method [Eurocode 8, NTC08] according to the distribution of the masses along the building height. However, there exists a variety of numerical procedures in the literature for designing the dissipative braces. The dissemination of different approaches and methodologies is motivated by the lack of a standardized design procedure in current European regulations [Eurocode 8, 2004]. Among these procedures, we mention force-based design approaches coupled with verification of the target deformation ex post [Ponzo et al., 2007; Ragni et al., 2010]; energy-based design procedures [Sorace and Terenzi, 2008; Choi and Kim, 2006; Foti and Nobile, 2012]; and displacement-based design approaches wherein the design starts from a target deformation [Kim and Choi, 2006; Priestley et al., 2007]. The most popular methodologies are displacement-based design approaches that combine pushover analysis of the multi-degree-of-freedom (MDOF) structure with response spectrum analysis of an equivalent SDOF system under certain assumptions on the dissipative mechanisms. Among these, Mazza and Vulcano [Mazza and Vulcano, 2014; Mazza and Vulcano, 2015] developed an iterative displacement-based design procedure adopting a proportional stiffness criterion, in which the elastic lateral storey-stiffness due to the braces is assumed proportional to that of the unbraced frame. However, this method neglects the frame-damped brace interaction and, due to the proportional stiffness criterion, may produce a non-uniform distribution of storey drifts as the damper stiffness is distributed according to the

profile of the fundamental mode of vibration. As an alternative, Kasai et al. [Kasai and Ito, 2004; Ito and Kasai, 2006; JSSI, 2007; Pu and Kasai, 2012] proposed a rule (via closed form expressions) to arrange the damper stiffness along the building height so as to achieve a uniform distribution of interstory drifts. This method, originally conceived for steel structures, was later extended for retrofitting of existing RC structures with elastoplastic dampers [Sutcu et al., 2014; Takeuchi and Wada, 2017] and recently improved in an attempt to optimize the dimensions of the steel dampers at different storeys [Almeida et al., 2017].

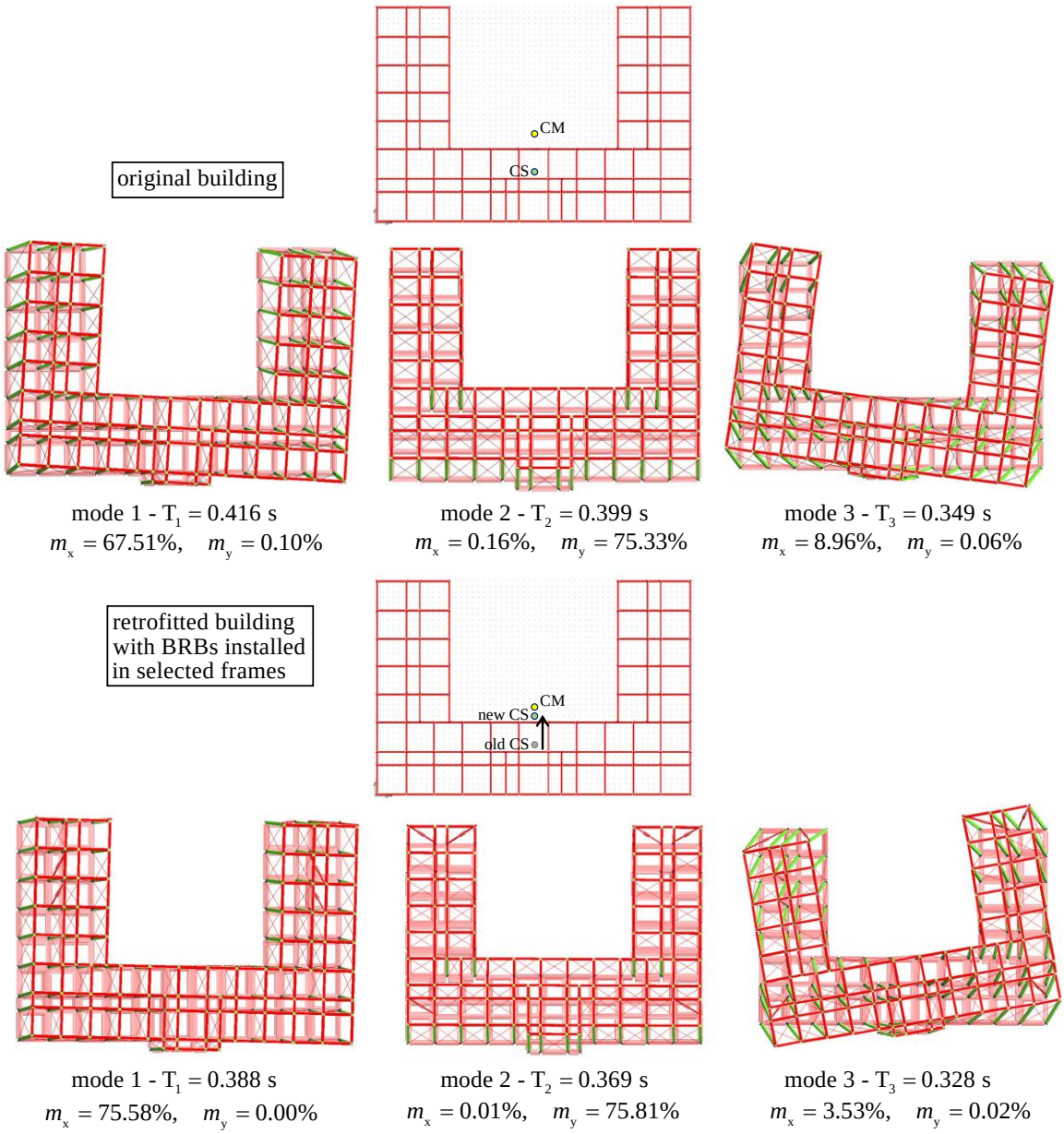


Figure 9 - *First three mode shapes of the existing building (top) and retrofitted building (bottom), with indication of the centre of mass (CM), centre of stiffness (CS) and modal participating mass ratios in the two cases*

Table 7 – Periods, modal masses and participating mass ratios for the existing building

| mode # | periods (s) | $M_x$ (t) | $M_y$ (t) | $m_{x,cumulated}$ (%) | $m_{y,cumulated}$ (%) |
|---|---|---|---|---|---|
| 1 | 0.416 | 4341.7 | 6.58 | 67.51 | 0.10 |
| 2 | 0.399 | 10.1 | 4845.04 | 67.66 | 75.44 |
| 3 | 0.349 | 576.19 | 3.6 | 76.62 | 75.49 |
| 4 | 0.209 | 0 | 798.27 | 76.62 | 87.90 |
| 5 | 0.186 | 371.88 | 0.03 | 82.41 | 87.90 |
| 6 | 0.184 | 486.25 | 0.03 | 89.97 | 87.90 |
| 7 | 0.148 | 0 | 349.14 | 89.97 | 93.33 |
| 8 | 0.145 | 0.39 | 4.01 | 89.97 | 93.40 |
| 9 | 0.129 | 250.47 | 0 | 93.87 | 93.40 |
| 10 | 0.095 | 210.86 | 49.43 | 97.14 | 94.16 |
| 11 | 0.094 | 42.25 | 319.18 | 97.80 | 99.13 |
| 12 | 0.089 | 76.29 | 2.65 | 98.99 | 99.17 |

Table 8 – Periods, modal masses and participating mass ratios for the retrofitted building

| mode # | periods (s) | $M_x$ (t) | $M_y$ (t) | $m_{x,cumulated}$ (%) | $m_{y,cumulated}$ (%) |
|---|---|---|---|---|---|
| 1 | 0.388 | 4860.9 | 0.14 | 75.58 | 0.00 |
| 2 | 0.369 | 0.42 | 4875.78 | 75.59 | 75.81 |
| 3 | 0.329 | 227.03 | 1.52 | 79.12 | 75.84 |
| 4 | 0.198 | 0 | 664.22 | 79.12 | 86.16 |
| 5 | 0.177 | 93.54 | 0.03 | 80.57 | 86.17 |
| 6 | 0.169 | 555.49 | 0 | 89.21 | 86.17 |
| 7 | 0.136 | 0.02 | 513.26 | 89.21 | 94.15 |
| 8 | 0.128 | 0.76 | 0.76 | 89.22 | 94.16 |
| 9 | 0.124 | 420.84 | 0.01 | 95.76 | 94.16 |
| 10 | 0.088 | 0 | 303.15 | 95.76 | 98.87 |
| 11 | 0.085 | 253.91 | 0.04 | 99.71 | 98.87 |
| 12 | 0.081 | 9.77 | 1.24 | 99.86 | 98.89 |

Some drawbacks of this approach were pointed out by Ferraioli and Lavino [Ferraioli and Lavino, 2018] and are here briefly recalled. First, this approach neglects the interaction effects between the damped braces and the RC frame, primarily, the increase of axial loads induced by the damped braces, which may cause overstressing of columns and premature failure modes (this was also noted in the context of dissipative braces with fluid viscous dampers [Karavasilis, 2016; De Domenico et al., 2019]). Second, this approach is very sensitive to the distribution of the frame stiffness along the building height, which typically decreases passing from bottom to top. As a consequence, it might produce a concentration of shear forces in the first storey columns (where, ideally, negative values of optimal damper stiffness may be obtained, meaning that no dampers should be inserted according to the closed form expression). To overcome these drawbacks, Ferraioli and Lavino [Ferraioli and Lavino, 2018] developed an improved variant of the Mazza and Vulcano [Mazza and Vulcano, 2015] direct displacement-based design procedure incorporating frame-damper interactions and higher modes contributions (by

using an adaptive pushover analysis), which accounts for torsion effects in asymmetric buildings. The finite element model of the retrofitted building with BRBs is shown in Figure 10, along with some sketches on the main assumptions regarding the force-displacement curve (idealized bilinear model) of the hysteretic dampers. The stiffness of the BRBs results from a "series spring model" incorporating both the stiffness of the brace $k_b$ and the elastic stiffness of the hysteretic damper $k_d = F_y / u_y$.

As a preliminary design criterion, the rule of thumb of BRBs absorbing the 40% of the earthquake-induced lateral force at each floor is adopted. Two types of hysteretic dampers have been selected: type 1 dampers, adopted for the first three elevations, are characterized by yield displacement $d_y = 1.63$ mm, yielding force $F_y = 737$ kN, ultimate displacement $d_u = 15$ mm and corresponding ultimate force $F_u = 1065$ kN; type 2 dampers, adopted for the fourth and fifth elevation, are characterized by $d_y = 1.57$ mm, $F_y = 520$ kN, $d_u = 15$ mm and $F_u = 760$ kN.

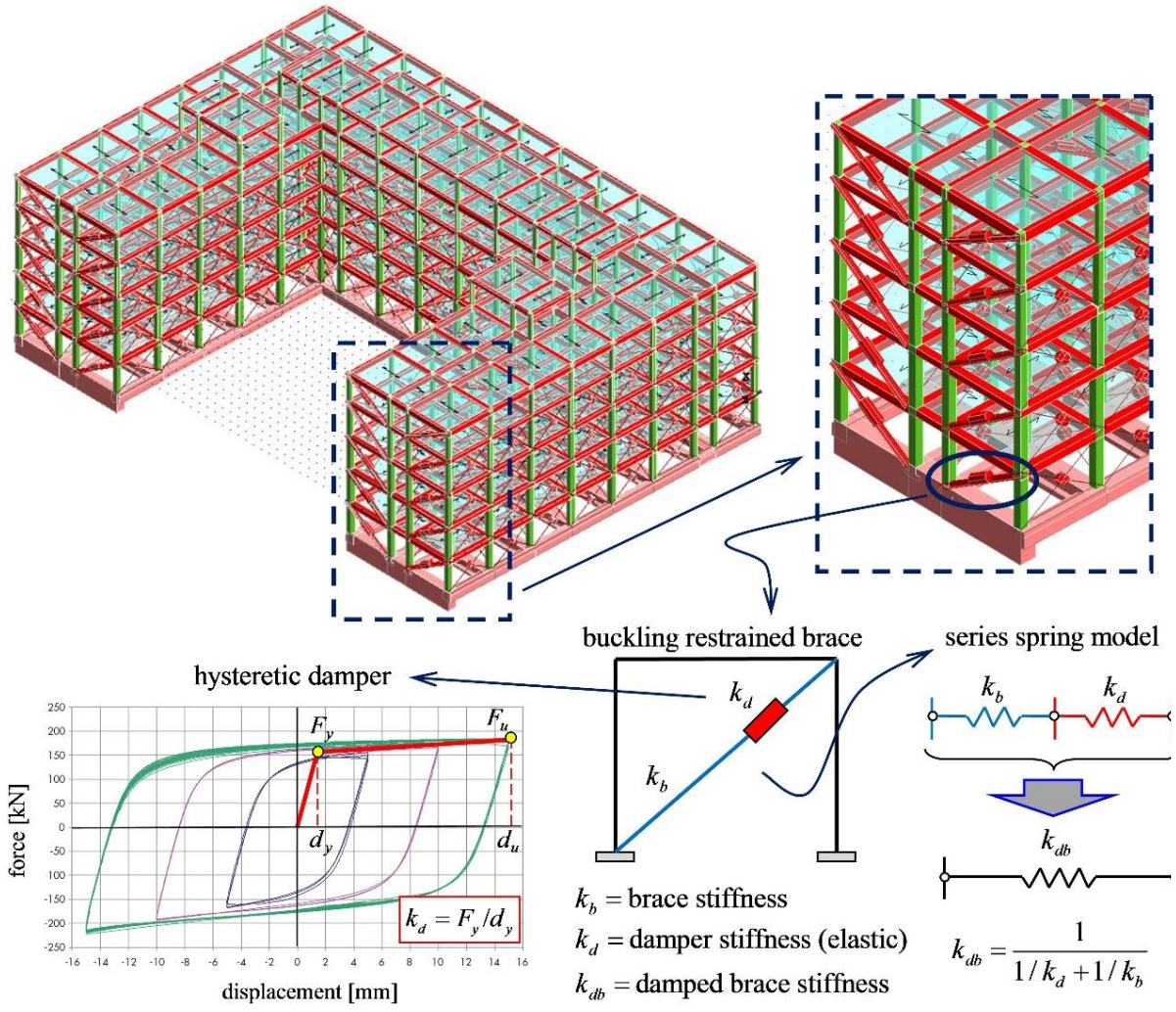


Figure 10 - *Finite element model of the retrofitted building with BRBs and simplified modeling assumptions for the force-displacement curve of the BRBs (bilinear model)*

It is worth pointing out that the yield displacement of less than 2 mm of the hysteretic dampers ensures that these supplemental energy dissipation devices be fully engaged even for small interstory drifts, as typically occurs in quite stiff masonry structures like the case study building.

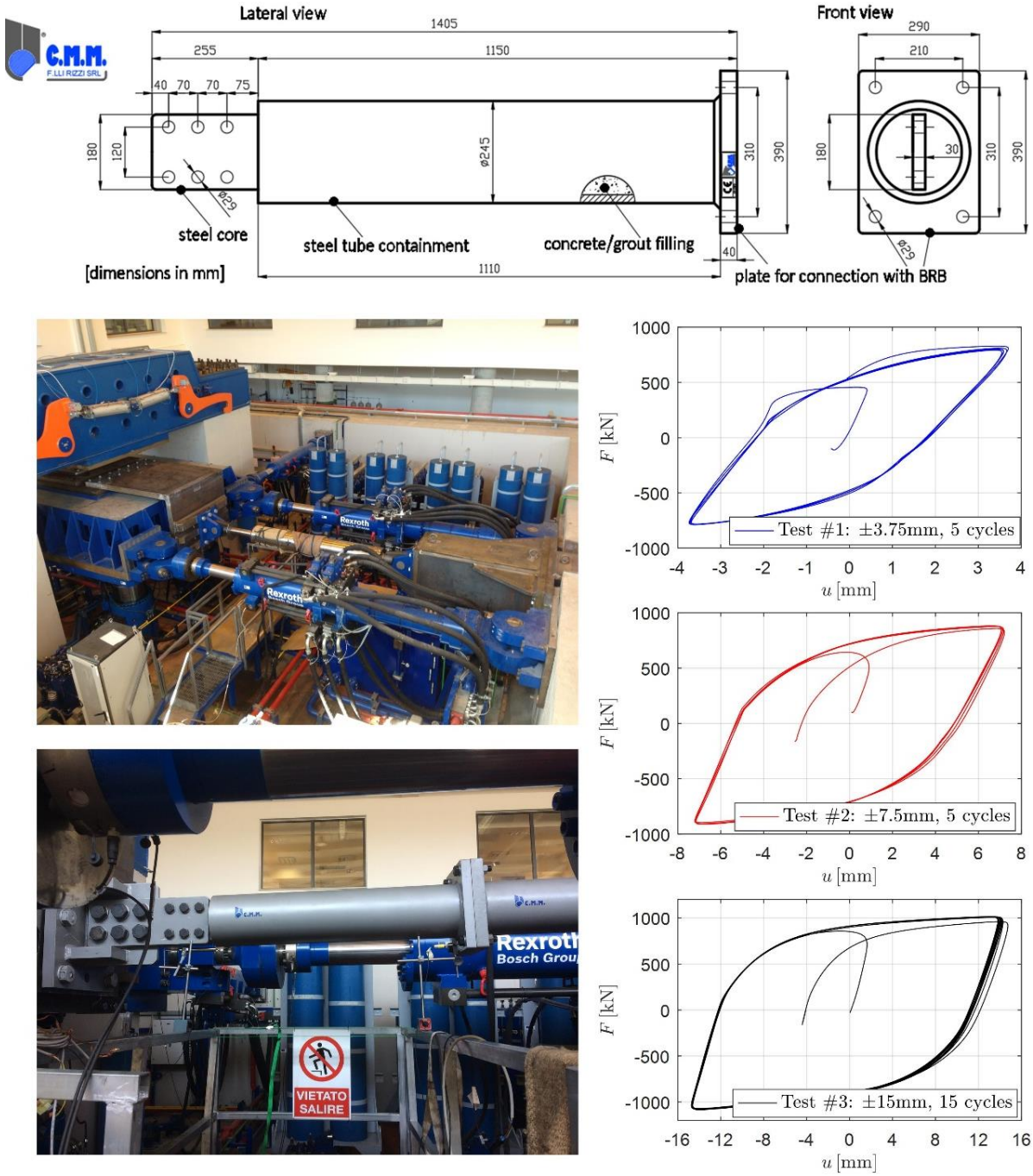


Figure 11 - *Acceptance tests, in accordance with UNI EN 15129:2009 regulations, on type 1 hysteretic damper carried out at the Eurolab of the CERISI, Messina, Italy*

The hysteretic dampers were produced by the Italian manufacturing company C.M.M. F.lli Rizzi s.r.l., and tested in accordance with the [UNI EN 15129:2009] (European regulations for antiseismic devices) as displacement-dependent (nonlinear) devices.
These tests were conducted at the Eurolab laboratory of the CERISI – Centre of Excellence Research and Innovation of Large Dimensions Structures and Infrastructures [Failla et al., 2015], located in Messina, Italy.
The testing equipment is endowed with two horizontal actuators (in the X axis – used for this experimental activity) having load capacity up to 3100 kN, stroke up to ±550 mm and allowing velocities up to 1100 mm/s. The damper is placed in between the horizontal actuators and a reaction wall, as shown in Figure 11. According to the [UNI EN 15129:2009] regulations, the tests were carried out at three different displacement levels:

- test #1 → 5 fully reversed cycles with amplitude $d_u / 4 = 3.75$ mm;
- test #2 → 5 fully reversed cycles with amplitude $d_u / 2 = 7.5$ mm;
- test #3 → 15 fully reversed cycles with amplitude $d_u = 15$ mm;

The experimental results for the type 1 hysteretic damper are reported in Figure 11. The experimental values of the hysteretic parameters ($d_y, F_y, d_u, F_u$) are in good agreement with the design parameters for the dampers adopted for the calculations, as reported above.
Additionally, specific construction details have been necessary to ensure proper connection between steel braces and existing masonry structure at all floors during the installation stages. The following steps have been envisaged in the design process, and performed during the actual construction works as documented by the photographs in Figure 12:

- removal of the existing masonry wall in the selected frame where the BRBs are to be installed;
- installation of connecting plates near the joints through threaded bars that penetrate the surrounding masonry structure and fixing through epoxy resin and anchoring bolts;
- placement of reinforcing steel frames (L-shaped steel elements welded to each other) and connection to the masonry structure through an additional set of threaded bars;
- installation of the BRB that is connected to the steel plates of the frame through bolts;

final closure with plasterboard (which can be easily removed whenever a visual inspection of the devices turns out to be necessary).

Nevertheless, some construction issues have emerged during the installation phases. These issues are mainly related to the slight misalignments of the RC beams from one floor to the above floor. These slights misalignments, which is related to a mistake during the earlier construction works of the existing building, have complicated the installation operations in ensuring proper alignments of the connecting threaded bars from one floor to the other without interfering with the steel bars of the existing RC beams. In some points of the structure, this has required to widen the holes for the placement of the connecting threaded bars, and subsequent filling with a liquid two-component (cement-polymer modified) self-compacting high-strength mortar to repair the defects on the concrete surfaces before coating.

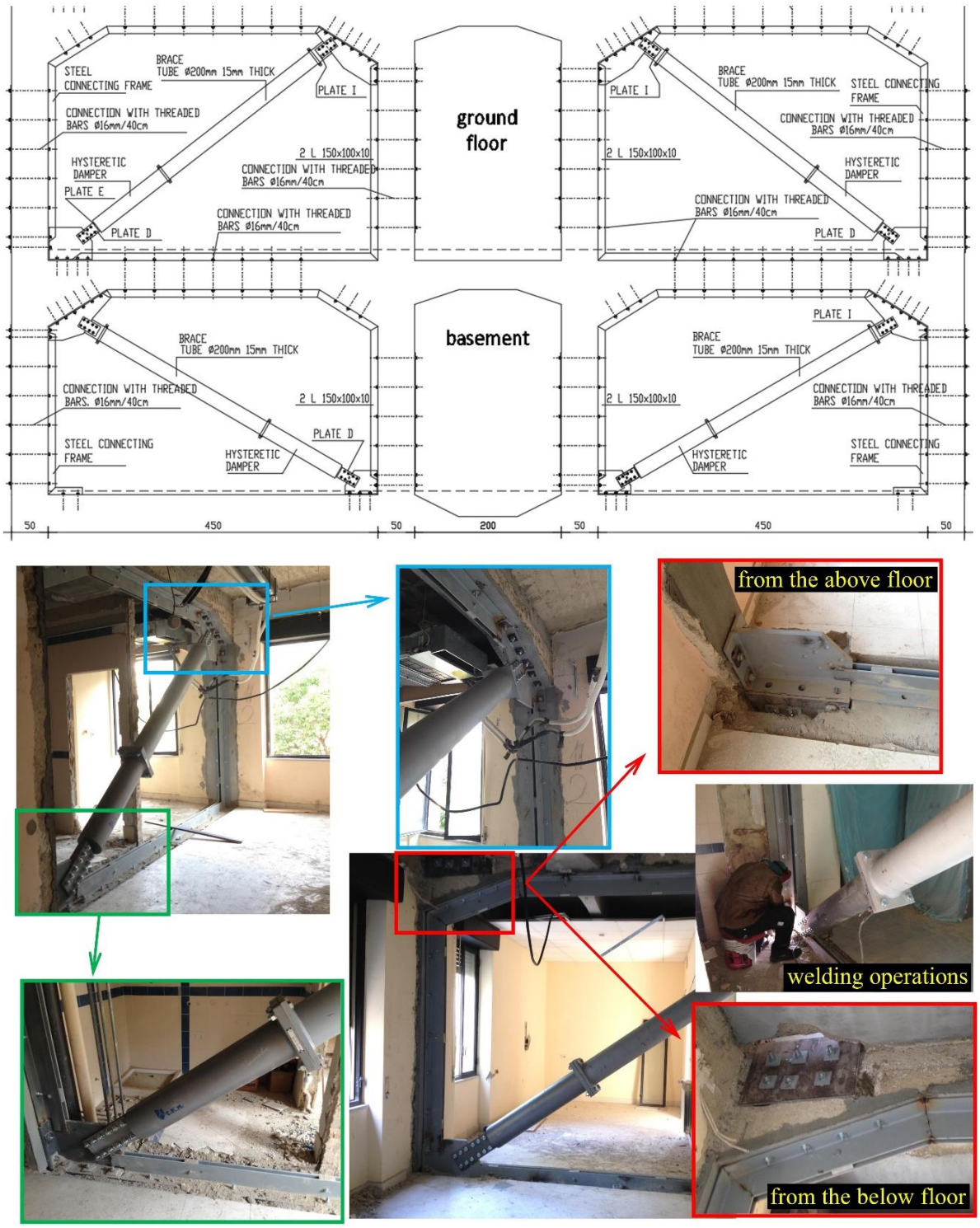


Figure 12 - *Design drawings detailing the connection of the hysteretic dampers and the masonry structure through added steel frames and photographs of installation stages*

## 4.2 Strengthening of beam-column joints through steel ribbons

A preliminary pushover analysis of the retrofitted building with BRBs revealed a more effective structural behavior, with interstory drifts limited to within 5% of the interstory height. In this way, the contribution of the masonry panels to the overall strength of the building is exploited in full. Moreover, it was found that the plastic deformations (flexural failures, of ductile type) first occur in RC beams and then in RC columns, which is quite in line with the capacity design principles and with the need of developing a global collapse mechanism. This is contrast to the previous pushover analysis results on the existing building (without retrofitting operations) in which shear failures (of brittle type) occurred in the foundations and in some RC beams of the structure.

Despite the improvements of the nonlinear structural behavior of the building, the structure with the BRBs still did not comply with the requirements prescribed by the Italian seismic code, as its capacity was found to be lower than the seismic demand. By carefully analyzing the progressive developments of plastic hinges occurring in the structure (here not reported for brevity), we have noted that, especially for the mode-distribution of the lateral loads, these plastic deformations are mainly concentrated in the beam-column joints of the last two elevations, namely the two floors realized in reinforced concrete that were added in a later stage (around 40 years later) than the original masonry building. Considering the different nature of the two materials (masonry versus RC), this result may be ascribed to the non-uniform distribution of stiffness in elevation, since the overlying RC frame behaves as a more flexible mass oscillating on the underlying more rigid masonry structure. Indeed, the displacement demand of the overall building is mostly concentrated in the more flexible floors of the last two elevations, which are therefore subject to larger plastic deformations.

Motivated by these preliminary observations, the goal of the retrofitting operations has been to ensure a proper structural connection between the added floors (RC frame) and the underlying confined masonry structure.

To this end, pre-tensioned stainless steel ribbons have been designed to strengthen the beam-column joints of the third floor by offering a beneficial triaxial compression stress state. In this way, the shear strength is increased and a more ductile flexural failure is promoted, in accordance with the capacity design principles. In particular, due to the presence of angular steel elements in all the corners of the section, the increase of shear strength is ensured in both the principal directions.

These angular steel elements are installed for a height of 100 cm above the beam-column joint between the second and third floor, as shown in the design drawings reported in Figure 13. The scheme of installation of the steel ribbons resembles that of the steel stirrups, as these strengthening elements are pre-tensioned (to provide a beneficial confinement action to the column) and placed at a predefined spacing (10 cm in the specific case, for an overall number of 10 steel ribbons in the strengthened zone). When the angular steel element are properly connected to the section, their contribution is also beneficial for improving the bending resistance.

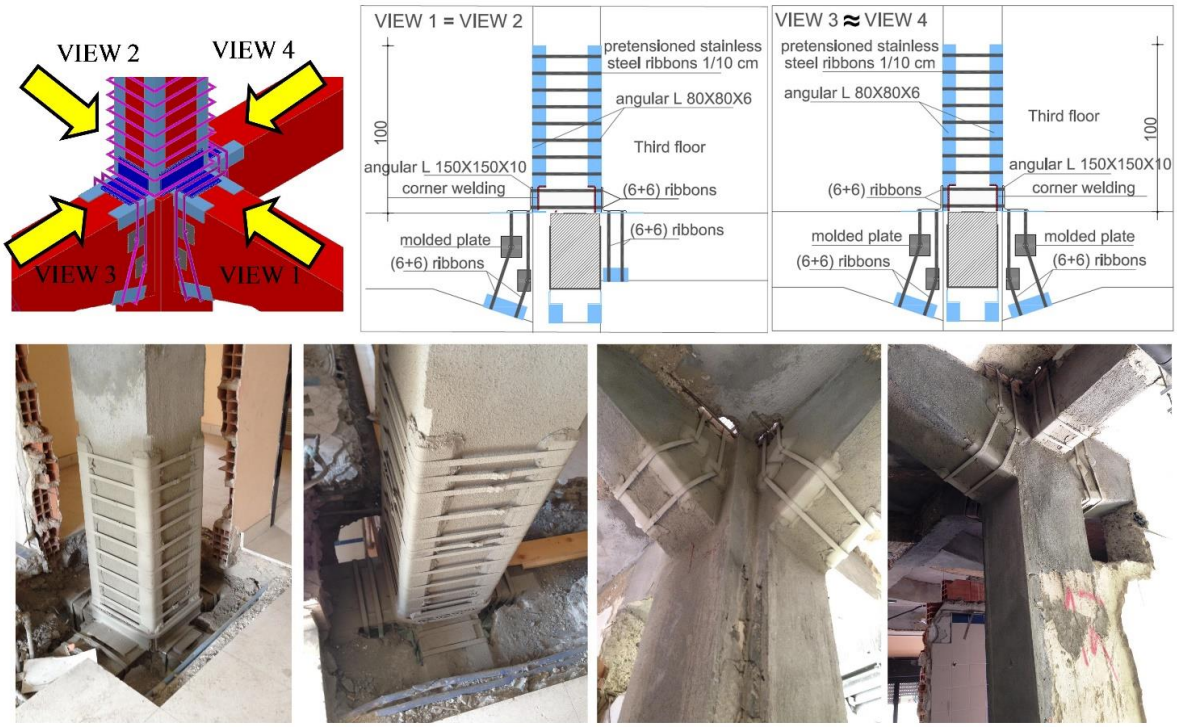


Figure 13 - *Design drawings and photographs of installation stages concerning the strengthening of the top-floor beam-column joint through pre-tensioned stainless steel ribbons*

According to the Italian seismic code [D.M. 2008, NTC 08], the contribution of this system to the shear strength can be considered to be additional to the existing strength (due to the original stirrups) provided the strengthened system remains in elastic stage. By limiting the steel stress to within 50% of its yield strength, the additional shear contribution provided by the steel ribbons $V_j$ can be computed as [D.M. 2008, NTC 08]

$$V_j = 0.5 \frac{2 t_j b}{s} d \; f_{yw} \frac{1}{\cos(\alpha_t)} \tag{6}$$

where $t_j$, $b$ and $s$ represent the thickness (0.9 mm), width (1.9 cm) and spacing of the steel ribbons (10 cm), $d$ is the section height, $f_{yw}$ is the yield stress of the steel (355 MPa) and $\alpha_t$ is the shear-induced crack inclination, assumed equal to 45°. The design of the strengthening system has been performed through a macro-element software package. Through expression (6) it has been evaluated that the additional shear contribution offered by the strengthening system is equal to 191 kN and 165 kN in the two main directions, respectively. Without strengthening system, the shear strength (due to the yielding shear reinforcement, $V_{RD,s}$) was equal to 86 kN and 75 kN. With the additional shear strengthening system, the global shear strength (due to the crushing of the compression struts, $V_{RD,max}$) became 197 kN and 195 kN, respectively for the two main directions. It emerges that for the two main directions the proposed strengthening system provides an increase of the shear strength equal to 197/86=2.3 and 195/75=2.6.

## 4.3 Pushover analysis of the retrofitted building

The structure has been re-analyzed through the pushover analysis, taking into account the retrofitting operations described above. The results for the two main directions and for the two load distributions along the building height (first-mode distribution and mass-proportional distribution) are reported in Figure 14 in the typical ADRS (acceleration-displacement response spectrum) format, in which both the structural capacity (pushover curve) and the demand spectra are indicated. It can be seen that the capacity of the retrofitted structure exceeds the seismic demand for both the damage-limitation requirement (SLD) and the no-collapse requirement (SLV). No shear failures were observed during the analysis. Moreover, plastic hinges formed firstly in the beams and, afterwards, in the columns according to the correct application of the capacity design principles. The most unfavourable results, among the 16 design scenarios are as follows: for SLD ("damage limitation requirement") the lowest ratio of the capacity PGA to design PGA is 1.089; for SLV ("no-collapse requirement") the lowest ratio of the capacity PGA to design PGA is 1.021. Consequently, in both cases the structure is safe since its displacement capacity is higher than the displacement demand, and these indicators increased significantly in comparison with the original (existing) building discussed above.

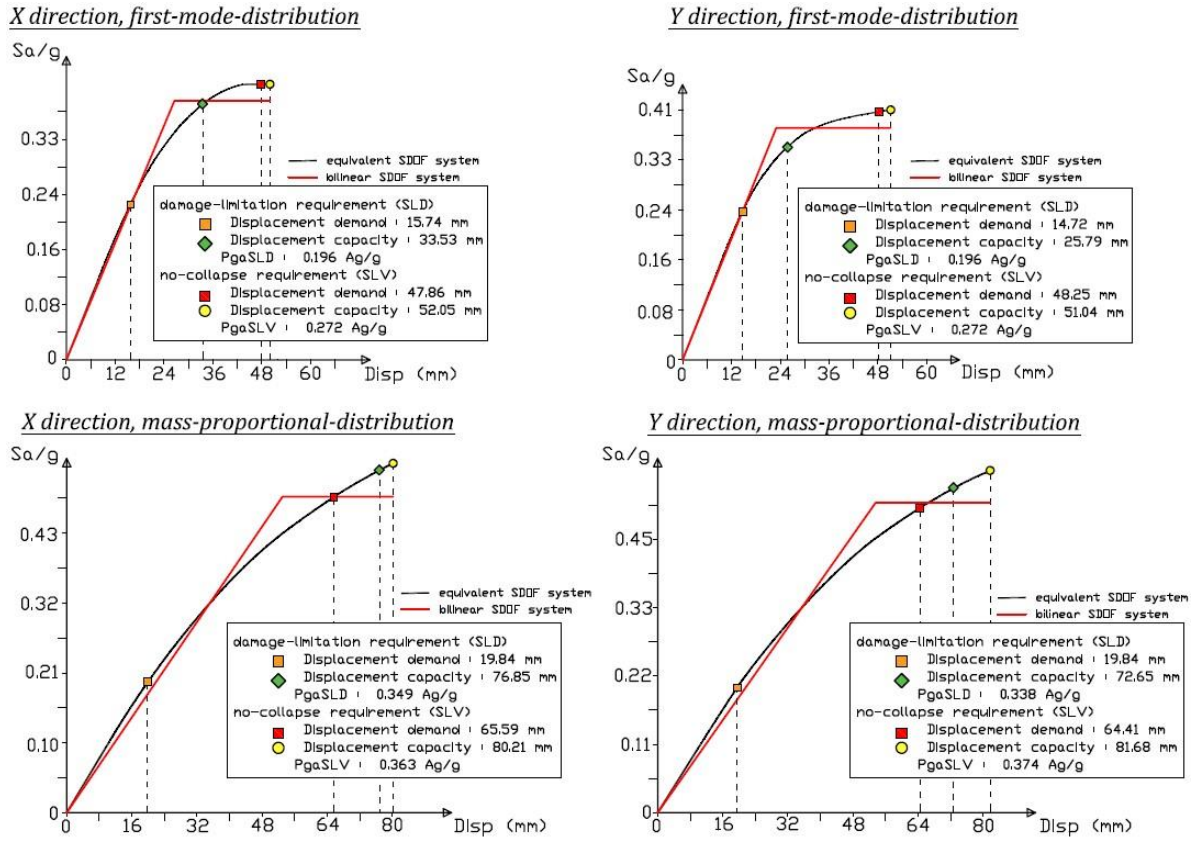


Figure 14 - *Pushover curves in acceleration-displacement format of retrofitted building for different loading scenarios*

The ratio of capacity PGA to design PGA gives indications of the safety index regarding ductile failure modes in terms of compatibility of displacements. Instead, according to § C 4.1.2.15 [D.M. 2008, NTC08] the safety index associated with brittle failure modes (e.g. shear failure of beams) in terms of comparison of strength values was found to be larger than 1.25 for all the design scenarios.
As a closure remark, it is worth noting that the present paper has analysed only one analysis method (pushover analysis) relying on common assumption of 5% damped demand spectra, which may be questionable due to the presence of hysteretic dampers. On the other hand, modifying these conventional assumptions based on a more appropriate level of effective damping from equivalent linearization procedures has not yet achieved universal consensus from the research community. In this regard, nonlinear response history analyses that incorporate the main nonlinearity effects (and the actual dissipation characteristics of the braces) represent an alternative, more detailed analysis method to assess the performance of the retrofitted building under study, and will be considered in future research work.

## 5 Concluding remarks

The present paper has focused on the seismic retrofitting intervention of a confined masonry-RC building analyzed as a case study, namely the university hall of residence of Messina, Italy. It was shown that this building presented, in its original configuration, high vulnerability to seismic action. The most important structural deficiencies of this building are summarized below:

- the foundation structures are inadequate to resist the design loads and fail due to shear forces;
- the building exhibits a moderate torsional behavior due to the asymmetry in one direction (along the *x* axis), which gives rise to higher stresses in the structural elements along the perimeter of the building;
- the building is non regular in elevation due to the presence of an added RC frame for the last two floors that was built in a later stage (almost 40 years later) than the underlying masonry building;
- the dissipation capacity of the building is unsatisfactory due to the very low transverse reinforcement amount in beams and columns and the absence of the capacity design principles at the time of construction (very low ductility of the existing building).

The retrofitting operations have addressed these specific critical aspects. In particular, the foundation has been retrofitted through a set of RC plates that have been added and connected to the existing inverted T-beams. This allows spreading the loads over a wider distribution area in a uniform manner. To minimize torsional effects and to increase the dissipation capacity of the building, buckling restrained braces have been designed and inserted in some frames as a replacement of the confined masonry walls. These frames have been specifically selected with the aim to align (as much as possible) the centre of mass with the centre of stiffness. These hysteretic dampers are particularly suitable for this (quite stiff) building because their yield displacement is of few millimetres, thus they are engaged even for small interstory drifts and provide satisfactory energy dissipation capacity. Finally, the beam-column joints of the third floor have been reinforced through pre-tensioned stainless steel ribbons. This turns out to be necessary since these zones are particularly critical due to the different nature of the RC frame

at the fifth elevation (third story), added in a later stage than the original structure, in comparison with the underlying masonry building. This RC frame behaves as a more flexible mass oscillating on the underlying more rigid masonry structure, thus absorbing larger deformations.
The set of retrofitting interventions described above has led to a considerable improvement of the seismic performance of the building. The retrofitted building now complies with the seismic requirements of the Italian seismic code, both in terms of damage limitation requirement (SLD) and no-collapse requirement (SLV). Although limited to the discussion of a specific case study, in the authors' opinion these retrofitting operations are feasible and applicable to a vast range of buildings constructed around a half century ago in other municipalities and having similar structural configurations and materials.

## References

Al-Chaar, G. (2002). Evaluating Strength and Stiffness of Unreinforced Masonry Infill Structures, No. ERDC/CERL-TR-02-1, Engineer Research and Development Center, Construction Engineering Research Lab, Champaign, IL, USA.

Almeida, A., Ferreira, R., Proença, J.M., Gago, A.S. (2017). Seismic retrofit of RC building structures with Buckling Restrained Braces. Engineering Structures; 130: 14-22.

Amato, G., Cavaleri, L., Fossetti, M., Papia, M. (2008). Infilled frames: influence of vertical loads on the equivalent diagonal strut model. In: Proceedings of 14th WCEE, CD-ROM, Beijing, China.

Asteris, P.G., Antoniou, S.T., Sophianopoulos, D.S., Chrysostomou, C.Z. (2011). Mathematical macro-modeling of infilled frames: state-of-the-art. ASCE Journal of Structural Engineering; 137(12): 1508-1517.

Black, C.J., Makris, N., Aiken, I.D. (2004). Component testing, seismic evaluation and characterization of buckling-restrained braces. ASCE Journal of Structural Engineering; 130(6): 880-894.

Bruno, S., Valente, C. (2002). Comparative response analysis of conventional and innovative seismic protection strategies. Earthquake Engineering and Structural Dynamics; 31(5): 1067-1092.

Castaldo, P., Palazzo, B., Della Vecchia, P. (2015). Seismic reliability of base-isolated structures with friction pendulum bearings. Engineering Structures, 95, 80-93.

Cavaleri, L., Fossetti, M., Papia, M. (2005). Infilled frames: Developments in the evaluation of the cyclic behaviour under lateral loads. Structural Engineering and Mechanics; 21: 469-494.

Choi, H., Kim, J. (2006). Energy-based seismic design of buckling-restrained braced frames using hysteretic energy spectrum. Engineering Structures; 28(2): 304-311.

Circolare Ministeriale 10/4/1997 n. 65 - Istruzioni per l'applicazione delle "Norme tecniche per le costruzioni in zone sismiche" di cui al decreto ministeriale 16 gennaio 1996 (in Italian).

Colajanni, P., Cacciola, P., Potenzone, B., Spinella, N., Testa, G. (2017). Non linear and linearized combination coefficients for modal pushover analysis. Ingegneria Sismica; 34(3-4): 93-112.

Crisafulli, F.J, Carr, A.J., Park, R. (2000). Analytical modelling of infilled frame structures - a general review, Bull. New Zealand Soc. Earthquake Eng.; 33(1): 30-47.

Crisafulli, F.J., Carr, A.J. (2007). Proposed macro-model for the analysis of infilled frame structures. Bull. New Zealand Soc. Earthquake Eng.; 40(2): 69-77.

De Domenico, D., Ricciardi, G. (2018a). Earthquake-resilient design of base isolated buildings with TMD at basement: Application to a case study. Soil Dynamics and Earthquake Engineering; 113: 503-521.

De Domenico, D., Ricciardi, G. (2018b). Optimal design and seismic performance of tuned mass damper inerter (TMDI) for structures with nonlinear base isolation systems. Earthquake Engineering and Structural Dynamics; 47(12): 2539-2560.

De Domenico, D., Ricciardi, G., Benzoni, G. (2018a). Analytical and finite element investigation on the thermo-mechanical coupled response of friction isolators under bidirectional excitation. Soil Dynamics and Earthquake Engineering, 106, 131-147.

De Domenico, D., Falsone, G., Ricciardi, G. (2018b). Improved response-spectrum analysis of base-isolated buildings: A substructure-based response spectrum method. Engineering Structures; 162: 198-212.

De Domenico, D., Falsone, G., Laudani, R. (2018c). In-plane response of masonry infilled RC framed structures: A probabilistic macromodeling approach. Structural Engineering and Mechanics; 68(4): 423-442.

De Domenico, D., Ricciardi, G. (2019). Earthquake protection of structures with nonlinear viscous dampers optimized through an energy-based stochastic approach. Engineering Structures; 179: 523-539.

De Domenico, D., Ricciardi, G., Takewaki, I. (2019). Design strategies of viscous dampers for seismic protection of building structures: A review. Soil Dynamics and Earthquake Engineering; 118: 144-165.

De Stefano, M., Pintucchi, B. (2008). A review of research on seismic behaviour of irregular building structures since 2002. Bulletin of Earthquake Engineering; 6(2): 285-308.

Decanini, L.D., Fantin, G.E. (1987). Modelos simplificados de la mampostería incluida en porticos. Características de rigidez y resistencia lateral en astado límite, In: Proceedings of the Jornadas Argentinas de Ingenierìa Estructural.

Di Sarno, L., Manfredi, G. (2010). Seismic retrofitting with buckling restrained braces: Application to an existing non-ductile RC framed building. Soil Dynamics and Earthquake Engineering; 30(11): 1279-1297.

EN 15129. (2009). Antiseismic devices. Brussels: Comité Européen de Normalisation (CEN).

European Committee for Standardization. Eurocode 8 - design of structures for earthquake resistance. part 1: General rules, seismic actions and rules for buildings; 2004.

Failla, I., Fazzari, B., Ricciardi, G., Stella, A. (2015). The Eurolab anti-seismic device (ASD) test facility at the University of Messina – Italy. In: Proceedings of the 14th world conference on seismic isolation. San Diego, CA, USA; 2015.

Fajfar, P. (2000). A nonlinear analysis method for performance based seismic design. Earthquake Spectra; 16(3): 573-592.

Ferraioli, M., Lavino, A. (2018). A Displacement-Based Design Method for Seismic Retrofit of RC Buildings Using Dissipative Braces", Mathematical Problems in Engineering, vol. 2018, Article ID 5364564, (2018). https://doi.org/10.1155/2018/5364564.

Ferraioli, M., Lavino, A., Mandara, A. (2016). An adaptive capacity spectrum method for estimating seismic response of steel moment-resisting frames. Ingegneria Sismica; 1-2: 47-60.

Ferraioli, M., Lavino, A., Mandara, A. (2018). Effectiveness of multi-mode pushover analysis procedure for the estimation of seismic demands of steel moment frames. Ingegneria Sismica; 35(2): 78-90.

Ferraioli, M., Mandara A. (2016). Base Isolation for Seismic Retrofitting of a Multiple Building Structure: Evaluation of Equivalent Linearization Method. Mathematical Problems in Engineering; vol. 2016.

Ferraioli, M., Mandara, A. (2017). Base Isolation for Seismic Retrofitting of a Multiple Building Structure: Design, Construction, and Assessment. Mathematical Problems in Engineering, vol. 2017.

Foti, D., Nobile, R. (2012). Optimum design of a new hysteretic dissipater. Des Optim Active Passiv Struct Control Syst; 1: 274-299.

Gandelli, E., Quaglini, V., Dubini, P., Limongelli, M.P., Capolongo, S. (2018). Seismic isolation retrofit of hospital buildings with focus on non-structural components. Ingegneria Sismica; 35(4): 20-56.

Italian Ministry of Infrastructure. Nuove norme tecniche per le costruzioni (NTC08). In Italian; 2008.

Ito, H., Kasai, K. (2006). Passive control design for elasto-plastically damped building structure. In: Proceedings of STESSA 2006 – Mazzolani & Wada (eds), Wada. Mazzolani, Ed., Taylor & Francis Group, London, 2006.

JSSI Manual 2nd Edition, Design and Construction Manual for Passively Controlled Buildings, Japan Society of Seismic Isolation (JSSI), Tokyo, Japan, 2007.

Karavasilis, T.L. (2016). Assessment of capacity design of columns in steel moment resisting frames with viscous dampers. Soil Dynamics and Earthquake Engineering; 88: 215-222.

Kasai, K., Ito, H. (2004). JSSI Manual for building passive control technology Part-8 peak response evaluation and design for elasto-plastically damped system. In: Proceedings of 13th World Conference on Earthquake Engineering, Vancouver, B.C., Canada, 2004.

Kent, D.C., Park, R. (1971). Flexural members with confined concrete. Journal of the Structural Division, ASCE 1971; 97: No. ST7, Proc. Paper 8243, pp. 1969-1990.

Kersting, R.A., Fahnestock, L.A., López, W.A. (2015). Seismic Design of Steel Buckling-Restrained Braced Frames. NEHRP Seismic Design Technical Brief No. 11, NIST GCR; 15-917.

Kim, J., Choi, H. (2006). Displacement-based design of supplemental dampers for seismic retrofit of a framed structure. ASCE Journal of Structural Engineering; 132(6): 873-883.

Kreslin, M. and Fajfar, P. (2012). The extended N2 method considering higher mode effects in both plan and elevation. Bulletin of Earthquake Engineering; 10(2): 695-715.

Longo, A., Montuori, R., Piluso, V. (2015). Seismic design of chevron braces cupled with MRF fail safe systems. Earthquakes and Structures, 8(5), 1215-40.

Mazza, F., Vulcano, A. (2014). Design of hysteretic damped braces to improve the seismic performance of steel and rc framed structures. Ingegneria Sismica; 31(1): 5-16.

Mazza, F., Vulcano, A. (2015). Displacement-based design procedure of damped braces for the seismic retrofitting of rc framed buildings. Bulletin of Earthquake Engineering; 13(7): 2121-2143.

Oliveto, G., Marletta, M. (2005). Seismic retrofitting of reinforced concrete buildings using traditional and innovative techniques. ISET Journal of Earthquake Technology; 42(2-3): 21-46.

Polyakov, S.V. (1960). On the Interaction between Masonry Filler Walls and Enclosing Frame When Loading in the Plane of the Wall. Translations in Earthquake Engineering, EERI, Oakland, CA, 36-42.

Ponzo, F.C., Dolce, M., Di Cesare, A., Vigoriti, G., Arleo, G. (2007). A design procedure for energy dissipating displacement-dependent bracing system for r/c buildings. In: Proceedings of the 10th world conference on seismic isolation, energy dissipation and active vibrations Control of Structures, Istanbul, Turkey.

Priestley, M.J.N., Calvi, G.M., Kowalsk, M.J. (2007). Displacement-based design of structures. Istituto Universitario di Studi Superiori di Pavia, Pavia, Italy, 2007.

Pu, W., Kasai, K. (2012). Design Method for RC Building Structure Controlled by Elasto-Plastic Dampers Using Performance Curve. In: Proceedings of the 15th World Conference on Earthquake Engineering, Lisbon, Portugal, 2012.

Ragni, L., Zona, A., Dall'Asta, A. (2010). Response sensitivity analysis of steel frames with buckling-restrained braces. In: Proceedings of the 14th European conference on earthquake engineering, Skopije, Macedonia, paper no 1738.

Regio Decreto Legge 23 Ottobre 1924 n. 2089 – R.D. n. 2089 (in Italian).

Sabelli, R., Mahin, S., Chang, C. (2003). Seismic demands on steel braced frame buildings with buckling-restrained braces. Engineering Structures; 25(5): 655-666.

Scott, B.D., Park, R., Priestley, M.J.N. (1982). Stress-strain behavior of concrete confined by overlapping hoops at low and high strain rates. ACI Journal; 79(6): 496-498.

Soong, T.T., Dargush, G.F. (1997). Passive energy dissipation systems in structural engineering. Chichester: John Wiley & Sons.

Sorace, S., Terenzi, G. (2001). Non-linear dynamic modelling and design procedure of FV spring-dampers for base isolation. Engineering Structures; 23(12): 1556–1567.

Sorace, S., Terenzi, G. (2008). Seismic protection of frame structures by fluid viscous damped braces. J Struct Eng ASCE; 134(1): 45-55.

Spencer Jr., B.F., Nagarajaiah, S. (2003). State of the art of structural control. ASCE Journal of Structural Engineering; 129(7): 845-856.

Sutcu, F., Takeuchi, T., Matsui, R. (2014). Seismic retrofit design method for RC buildings using buckling-restrained braces and steel frames. Journal of Constructional Steel Research; 101: 304-313.

Symans, M. D., Charney, F. A., Whittaker, A. S., Constantinou, M. C., Kircher, C. A., Johnson, M. W., & McNamara, R. J. (2008). Energy dissipation systems for seismic applications: current practice and recent developments. ASCE Journal of Structural Engineering, 134(1), 3-21.

Takeuchi, T., Wada, A. (2017). Buckling-Restrained Braces and Applications, Japan Society of Seismic Isolation (JSSI), Tokyo, Japan, 2017.

Tarque, N., Candido, L., Camata, G., Spacone, E. (2015). Masonry infilled frame structures: State-of-the-art review of numerical modelling. Earthquakes and Structures; 8(3): 731-757.

Tremblay, R., Bolduc, P., Neville, R., DeVall, R. (2006). Seismic testing and performance of buckling restrained bracing systems. Canadian Journal of Civil Engineering; 33: 183-198.

Tubaldi, E., Barbato, M., Dall'Asta, A. (2014). Performance-based seismic risk assessment for buildings equipped with linear and nonlinear viscous dampers. Engineering Structures; 126:90–99.

Wada, A., Nakashima, M. (2004). From infancy to maturity of buckling restrained braces research. Proceedings of the 13th World Conference on Earthquake Engineering, Vancouver, Canada, 2004.

Watanabe, A., Hitomi, Y., Saeki, E., Wada, A., Fujimoto, M. (1988). Properties of brace encased in buckling-restraining concrete and steel tube. Proceedings of the 9th World Conference on Earthquake Engineering, Tokyo-Kyoto, Japan, 1988.

Xie, Q. (2005). State of the art buckling-restrained braces in Asia. Journal of Constructional Steel; 61 (6), pp. 727-748.

Zhou, X., Yan, W., Yang, R. (2002). Seismic base isolation, energy dissipation and vibration control of building structures. Jianzhu Jiegou Xuebao/Journal of Building Structures; 23(2): 2-13.

ingegneria sismica
International Journal of Earthquake Engineering
Anno XXXVI – Num.1

# ADEGUAMENTO SISMICO DI EDIFICI IN MURATURA CONFINATA E CEMENTO ARMATO COLLABORANTE: IL CASO STUDIO DELLA CASA DELLO STUDENTE DI MESSINA, ITALIA

*Dario De Domenico*[1], *Nicola Impollonia*[2], *Giuseppe Ricciardi*[1]

[1] Department of Engineering, University of Messina, Italy

[2]Department of Civil Engineering and Architecture, University of Catania, Italy

SUMMARY: Molti edifici in territori ad alto rischio sismico furono progettati con normative obsolete e non soddisfano gli standard prestazionali attuali. Questo richiede strategie di adeguamento sismico efficaci. Dopo il collasso della casa dello studente a L'Aquila, Italia, nel 2009, numerose autorità locali e regionali in altre città italiane hanno programmato delle campagne di indagine per effettuare valutazioni sismiche di edifici destinati ad alloggi universitari simili, evidenziando in molti casi drammatiche deficienze strutturali. Uno di questi casi riguarda la casa dello studente di Messina, edificio in muratura animata collaborante trattato in questo articolo. Questo lavoro riassume la concezione teorica e la filosofia progettuale che ha animato questo intervento di adeguamento sismico (con controventi dissipativi ad instabilità impedita e incamiciatura dei nodi trave-pilastro con nastri in acciaio pretensionati), descrive i test di accettazione sugli smorzatori isteretici effettuati al laboratorio CERISI di Messina e discute alcune problematiche di costruzione che sono emerse durante le fasi di installazione fino ad oggi.

KEYWORDS: *adeguamento sismico, dissipatori isteretici, controventi dissipativi ad instabilità impedita, tecnologia CAM (incamiciatura con nastri in acciaio pretensionati), edificio con muratura confinata*

Corresponding author: Dario De Domenico, Department of Engineering, University of Messina, Italy.
Email: dario.dedomenico@unime.it